

# Recent Advances in Cleaner Hydrogen Productions via Thermocatalytic Decomposition of Methane: Admixture with Hydrocarbon

Anuar Faua'ad Syed Muhammad<sup>1</sup>, Ali Awad<sup>2</sup>, R. Saidur<sup>3,4</sup>, Nurliyana Masiran<sup>2</sup>, Md. Abdus Salam<sup>5</sup>, Bawadi Abdullah<sup>\*2,6</sup>

<sup>1</sup>Bioprocess and Polymer Engineering Department, Faculty of Chemical and Energy Engineering, Universiti Teknologi Malaysia, 81310 UTM Skudai, Johor, Malaysia

<sup>2</sup>Chemical Engineering Department, Universiti Teknologi PETRONAS, 32610 Seri Iskandar, Malaysia

<sup>3</sup>Research Centre for Nano-Materials and Energy Technology (RCNMET), School of Science and Technology, Sunway University, Jalan University, 47500 Bandar Sunway, Selangor Malaysia

<sup>4</sup>Department of Engineering, Lancaster University, Lancaster, LA1 4YW, UK

<sup>5</sup>Hydrogen Energy Technology Laboratory, BCSIR Laboratories, Chittagong, Bangladesh

<sup>6</sup>CO<sub>2</sub> Utilization Group, Institute of Contaminant Management for Oil and Gas, Universiti Teknologi PETRONAS, 32610 Seri Iskandar, Malaysia

\* Corresponding author: bawadi\_abdullah@utp.edu.my, bawadi73@gmail.com, +6018-2310773

## Abstract

A continuous increase in the greenhouse gases concentration due to combustion of fossil fuels for energy generation in the recent decades has sparked interest among the researchers to find a quick solution to this problem. One viable solution is to use hydrogen as a clean and effective source of energy. In this paper, an extensive review has been made on the effectiveness of metallic catalyst in hydrocarbon reforming for CO<sub>x</sub> free hydrogen production via different techniques. Among all metallic catalyst, Ni-based materials impregnated with various transition metals as promoters exhibited prolonged stability, high methane conversions, better thermal resistance and improved coke resistance. This review also assesses the effect of reaction temperature, gas hour space velocity and metal loading on the sustainability of thermocatalytic decomposition TCD of methane. The practice of co-feeding of methane with other hydrocarbons specifically ethylene, propylene, hydrogen sulphide, and ethanol are classified in this paper with the detailed overview of TCD reaction kinetics over an empirical model based on power law that has been presented. In

33 addition, it is also expected that the outlook of TCD of methane for green hydrogen production  
34 will provide researchers with an excellent platform to the future direction of the process over Ni-  
35 based catalysts.

36 **Key Words:** Hydrogen production, Methane Conversion, Metallic Catalyst, Process Parameters,  
37 Co-Feeding, Reaction Kinetics

### 38 **Table of Contents**

39	Abstract.....	1
40	Key Words:.....	2
41	1. Introduction .....	3
42	1. Thermo-catalytic Decomposition (TCD) of CH <sub>4</sub> .....	7
43	2. Catalysts Involved in TCD .....	8
44	2.1. Mono Metallic Catalyst.....	8
45	2.2. Bi-Metallic Catalyst .....	16
46	2.3. Tri-metallic Catalyst.....	27
47	3. TCD Parameters .....	30
48	3.1. Reaction Temperature .....	30
49	3.2. Gas Hour Space Velocity .....	31
50	3.3. Metal loadings .....	32
51	4. TCD over admixtures as Feedstocks .....	35
52	4.1. Ethylene.....	36
53	4.2. Propylene.....	37
54	4.3. Hydrogen Sulphide.....	39
55	4.4. Ethanol.....	39
56	4.5. 2% Methanol/Methane .....	41
57	5. Kinetics and reaction mechanism of TCD .....	41
58	6. Outlook.....	47
59	7. Conclusion.....	48
60	Acknowledgement .....	49

61       References.....49

62

63       **1. Introduction**

64       The combustion of fossil fuels such as coal, oil, gasoline and natural gas satisfy the energy  
65       demands of industry and domestic users. However, they will run out momentarily due to the  
66       rapidly increasing demands [1]. Furthermore, the global warming, greenhouse effect, hole in ozone  
67       layer, acid rains and environmental pollution are the drastic effects caused by the fossil fuel  
68       combustion [2]. USA, Japan, and Germany are leading the race of CO<sub>2</sub> emissions as they have  
69       well stabilized industrial sectors [3]. The concentration of CO<sub>2</sub> in the atmosphere has increased  
70       drastically from 396 ppm to 400 ppm in recent few years. Moreover, it is estimated that these  
71       emissions will increase from 30 billion metric tons to 43 billion metric tons in 2035 [4]. The  
72       average temperature of the earth according to climate forecasts may increase from 274 to 279 K if  
73       the increasing greenhouse gas emissions are not critically considered. [5]. Extensive solutions have  
74       been reported by the researchers to reduce the hazardous effects of increasing concentration of  
75       CO<sub>2</sub> in the atmosphere by establishing various methods of CO<sub>2</sub> capture such as absorption,  
76       cryogenic and membrane processes [6]. Another method has been reported by using photo-  
77       catalytic reactors [7] to convert excessive CO<sub>2</sub> into useful products such as CH<sub>4</sub> and CH<sub>3</sub>OH. The  
78       invention of few high energy efficient green fuels that reduce the emissions of poisonous gases  
79       during combustion is also quoted as an active solution to control greenhouse effect. The search for  
80       alternative high energy efficient green fuels has been broadly investigated by many researchers in  
81       the past. H<sub>2</sub> has been termed as one of the greenest and lightest fuel that can fill in the energy gap  
82       which will be created in the upcoming future. Because of hydrogen’s abundance, lightweight, low  
83       mass density, high calorific value and non-polluting nature make it a unique source of energy.

84 Moreover, it has been published that H<sub>2</sub> has the highest heat of combustion, i.e. 142 kJ g<sup>-1</sup> as  
85 compared to petroleum and wood that exhibit 43-35 and 18 kJ g<sup>-1</sup> respectively [8].

86 The annual H<sub>2</sub> consumption in 2006 was around 50 million tons including industrial and domestic  
87 usage. Around 50% of this consumption was attributed to NH<sub>3</sub> industries, 37% in petroleum  
88 refineries, 7% in CH<sub>3</sub>OH production and 6% in other fields. It has been reported that the H<sub>2</sub>  
89 produced in existing date has to be multiplied 100 times approximately to meet the world's demand  
90 for fossil fuels presently [9]. It is believed that H<sub>2</sub> will play a vital role in fulfilling the extensive  
91 energy requirements. However, H<sub>2</sub> cannot be found freely in the atmosphere instead of in the form  
92 of bonds with other molecules that indicate its reactivity. Therefore, it must be extracted from other  
93 primary energy sources like coal, natural gas, water or other heavy hydrocarbons [10]. Global  
94 statistics illustrate that the significant amount of H<sub>2</sub> is being produced by the reforming of natural  
95 gas, i.e. 48%, electrolysis of water gives 30%, 18% from burning petroleum products and 4% by  
96 coal. The significant contribution to the production of H<sub>2</sub> is from natural gas since there are vast  
97 reservoirs of CH<sub>4</sub> in deep seabed especially in industrialized countries like United States [11].  
98 Natural gas has been named as the primary energy contributor since early 20's in Malaysia. In  
99 2008 alone, approximately over 2.5 trillion m<sup>3</sup> of the natural gas reserve were found in Malaysia  
100 specifically in Sarawak (East Malaysia). Moreover, the natural gas reserves in Malaysia are the  
101 largest in South East Asia and 12<sup>th</sup> largest around the globe [12].

102 There are various methods for the H<sub>2</sub> production such as; steam reforming (SRM), partial oxidation  
103 (POM), dry reforming (DRM) and thermocatalytic decomposition of CH<sub>4</sub> (TCD) [13-15]. Among  
104 these methods, POM, SRM, and DRM are considered as indirect methods of H<sub>2</sub> production. In  
105 these methods, CH<sub>4</sub> is treated with O<sub>2</sub>, H<sub>2</sub>O and CO<sub>2</sub> under given a set of reaction conditions to  
106 produce synthesis gas as a mixture of H<sub>2</sub> and CO [16]. However, there is a common shortcoming

107 in all these three processes in the form of emissions of greenhouse gases CO<sub>2</sub> and CO. These gases  
108 not only play a major role in global warming but also are very harmful when their mixed feedstock  
109 with H<sub>2</sub> is used in low-temperature fuel cells like proton exchange membrane fuel cells (PEMFC)  
110 [17].

111 Keeping in view the greenhouse gas emissions and its economic issues, the interest of researchers  
112 moved towards exploring a more optimum and green process for H<sub>2</sub> production. Thermocatalytic  
113 decomposition (TCD) is a practical approach to decompose CH<sub>4</sub> into H<sub>2</sub> and elemental carbon  
114 thermally. This method is considered novel and eco-friendly as there is no emission of greenhouse  
115 gases during the reaction [18].

116 Various review papers have been published in the past decades on this topic for example Jose et  
117 al. [19], Abbas et al. [9], Ashik et al. [20], Srilatha et al. [21], Sikander et al. [15] and Yongsan et  
118 al. [8-10]. Nonetheless, these reviews were limited on the TCD of CH<sub>4</sub> which heavily focussed on  
119 catalysts to reactor's type. In recent years, there are distinct works that are focussed on the  
120 feedstock combination with CH<sub>4</sub> [22, 23] which provide better conversions and improved the  
121 activity and stability of the catalysts. Thus, in this review, an attempt has been made to review on  
122 admixture feedstocks with CH<sub>4</sub> with other hydrocarbons critically. Moreover, this article also  
123 independently reviews on the type of catalysts, i.e. monometallic and multimetallic and their  
124 performances in TCD of CH<sub>4</sub>. We also highlighted the outlook of TCD in directing the future  
125 research in coming years. Fig. 1 shows a complete process that we take for this review article.

126

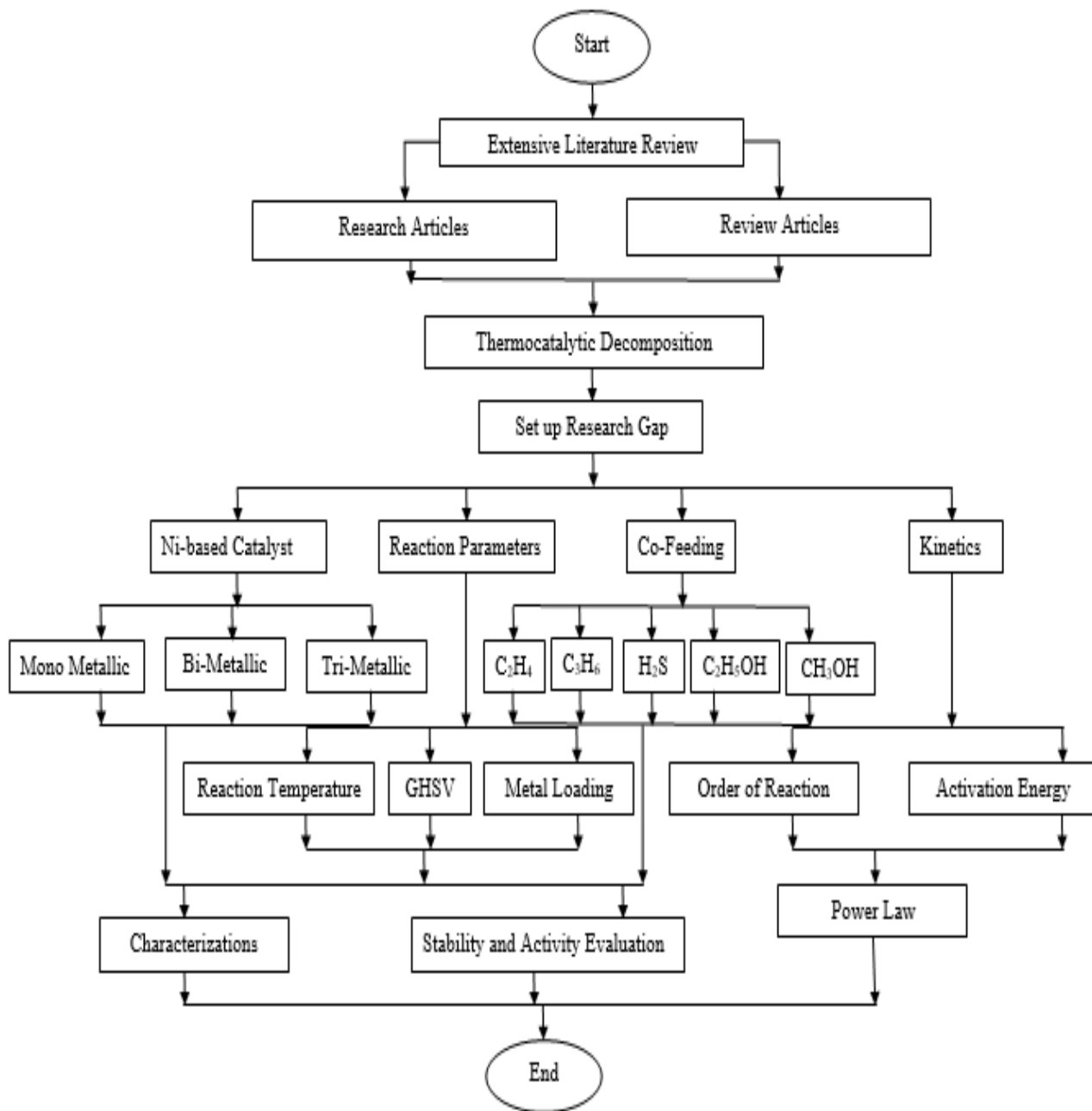
127

128

129

130

131



132

133

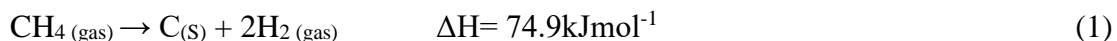
134

135

Fig 1: Process Flow of Review for TCD

136 **1. Thermo-catalytic Decomposition (TCD) of CH<sub>4</sub>**

137 TCD of CH<sub>4</sub> is a single step process which produces pure H<sub>2</sub> and carbon as a by-product [14]. This  
138 method is known as an eco-friendly process, and it has been extensively studied by various  
139 researchers [24]. The main advantages of TCD include the greenhouse free H<sub>2</sub> production that can  
140 be directly used in fuel cells and the production of CNF as a by-product [25]. The reaction proceeds  
141 as shown in Eqns. (1)–(6) [9].



142 The reaction occurs in four stages explained as:

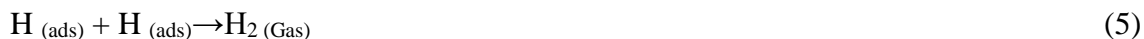
143 (a) In the first step, the CH<sub>4</sub> gets itself attached to the surface of the catalyst. The most  
144 important part of the catalyst contains the metal impregnated with suitable support and  
145 promoters.



146 (b) The breaking of sp<sup>3</sup> hybridized C-H bonds occurs. This is the most critical step since  
147 high energy is required to break strongly attached bonds.



148 (c) After the breakage of these bonds, the H converts into the molecular form thus  
149 becoming a primary product.



150 (d) The next step is the attachment of carbon on the surface of active sites. Hence, the  
151 active sites blocked, and the surface area of the catalyst is also decreased. Therefore, it  
152 is observed that the initial deactivation of the catalyst starts.



153 (e) The last step is the forming of carbon nuclei on the surface of the catalyst. Carbons get  
154 the form of MWCNT, CNF or BCNF depending upon nature and the operating  
155 conditions.

156 TCD is an endothermic reaction and occurs at high temperatures, i.e. 1473 K due to the highly  
157 stable tetrahedral structure of  $\text{CH}_4$  molecule supported by extremely stable C–H bonds with a bond  
158 energy of  $434 \text{ kJmol}^{-1}$ . Therefore, the applications of catalyst are mandatory to provide a robust  
159 pathway to decrease the activation energy [26]. To improve the reaction kinetics of TCD, Metal-  
160 based catalysts, and carbonaceous catalysts were introduced by numerous researchers. These  
161 include transition metal having partially filled d-orbital, activated carbon and carbon black [17].

## 162 **2. Catalysts Involved in TCD**

163 For commercially viable, the development of TCD process requires a low cost synthesized catalyst  
164 that results in higher and prolonged activities towards  $\text{CH}_4$  decomposition into  $\text{H}_2$  and elemental  
165 carbon. The literature survey on the study of the single metallic, bi-metallic and tri-metallic  
166 catalysts having different ratios in composition and synthesized by distinct techniques have been  
167 explained in Sections 2.1-2.3.

### 168 **2.1.Mono Metallic Catalyst**

169 Over the last few years, countless efforts have been made in the development of the preparation  
170 method of a suitable catalyst to optimize TCD of  $\text{CH}_4$  for  $\text{CO}_x$  free  $\text{H}_2$ . Various monometallic  
171 catalysts with different supports have been reported [27]. Apart from production of pure  $\text{H}_2$ , the  
172 invention of highly ordered carbon in the form of carbon nanofiber (CNF), carbon nanotubes  
173 (CNT), biwall carbon nanotubes (BWCNT), and multiwall carbon nanotubes (MWCNT) has been  
174 reported by researchers using these catalysts [28]. The morphology of the deposited carbon is

175 mainly dependent upon the metal loadings and reaction parameters. Although the general  
176 mechanism of TCD has been proposed to be similar for nearly all metallic materials, the catalytic  
177 stability and activity is influenced by catalysis synthesis techniques, pre-treatment of catalyst and  
178 most importantly the TCD parameters [24, 29]. Ni, Fe, and Co are the commonly used transition  
179 metals impregnated on Al<sub>2</sub>O<sub>3</sub>, SiO<sub>2</sub>, MgO and La<sub>2</sub>O<sub>3</sub> support [20].

180 Several investigators have reported productive work in bringing up the most optimized, reactive  
181 and stable catalysts for TCD of CH<sub>4</sub>. Ni-based materials are often stated as one of the most active,  
182 readily available and cost-effective catalysts for CH<sub>4</sub> reforming processes. It is reported that the  
183 performance of Ni-based catalysts is strongly dependent on the type of support it is impregnated  
184 on as the structure and electronic state of the catalyst changes once the material is successfully  
185 prepared. Therefore, it is worth mentioning that the best combination of Ni and apposite support  
186 can produce a highly active and stable catalyst for TCD of CH<sub>4</sub> [30]. Bayat et al. [31] studied  
187 various Ni loading on  $\gamma$ -Al<sub>2</sub>O<sub>3</sub> support. The results marked the catalysts as highly active and stable  
188 in the stated field of study, but they were sensitive to metal loadings and reaction temperatures.  
189 Owing to the endothermic nature of the reaction, the conversions of CH<sub>4</sub> increased periodically  
190 with reaction temperature. Moreover, it was also observed that at higher metal loadings the  
191 conversions were also high due to the presence of ample amounts of NiO on the surface of the  
192 support. The study done by Makvandi et al. [32] elaborated that the CH<sub>4</sub> conversions declined with  
193 TOS for Ni/Al<sub>2</sub>O<sub>3</sub> due to deposition of carbon on the active sites preventing the access of  
194 hydrocarbon. Moreover, the conversions increased linearly with metal loadings due to the  
195 availability of excessive active sites. The catalytic performance of 60% Ni/Al<sub>2</sub>O<sub>3</sub> was inspected by  
196 Ahmed et al. [33]. The results revealed that the textural properties play a vital role in the

197 performance of the catalyst since nanoparticle (NP) gave the highest yields as compared to the  
198 hollow sphere (HS) and bulk catalyst (BC).

199 Apart from  $\text{Al}_2\text{O}_3$  being the most studied by many researchers, studies on  $\text{MgO}$ ,  $\text{SiO}_2$ ,  $\text{TiO}_2$ ,  
200  $\text{MgAl}_2\text{O}_4$ ,  $\text{La}_2\text{O}_3$ , SBA-15, and  $\text{La}_2\text{O}_3$  have also been cited on Ni-based catalyst [34, 35]. The  
201 literature survey showed that Ni/ $\text{SiO}_2$  catalyst presented notable conversions, but eventually the  
202 catalyst deactivated due to the accumulation of carbon in the pores of the catalyst. TPO and TGA  
203 analysis supported the formation of MWCNT as a by-product [36].  $\text{TiO}_2$  was also reported to be  
204 active support for TCD of  $\text{CH}_4$  due to its high surface area and pore volume. This assisted in a fine  
205 dispersion of Ni creating vast amounts of NiO for  $\text{CH}_4$  breakage [37, 38]. All Ni support  $\text{TiO}_2$   
206 catalyst was highly active for  $\text{CH}_4$  decomposition reaction due to proper metal support interaction  
207 that also provided thermal stability to the catalyst.

208 Fe and Co-based materials are also classified as active metals for TCD of  $\text{CH}_4$ . Besides Ni. Pinilla  
209 and co-workers [39] came up with results which showed that high  $\text{CH}_4$  conversions are allowed  
210 by Fe based catalyst at operating temperatures higher than 1073 K. The researchers also compared  
211 the catalytic efficiency of  $\text{Al}_2\text{O}_3$  and  $\text{MgO}$  supports and ranked Fe impregnated on prior support as  
212 more stable compared to later one. The influence of metal loading and the effects of support on Fe  
213 based catalyst was again discussed briefly in [40]. Fe catalyst supported on  $\text{Al}_2\text{O}_3$  showed high  
214 conversions as compared to  $\text{MgO}$  and  $\text{TiO}_2$ . The catalytic order w.r.t. support was as  $\text{Al}_2\text{O}_3 > \text{MgO}$   
215  $> \text{TiO}_2$ . The performance of Fe supported on  $\text{Al}_2\text{O}_3$  as an active catalyst for TCD of  $\text{CH}_4$  was also  
216 acknowledged by [41]. The study of Ibrahim et al. [28] also justified that the  $\text{CH}_4$  conversions  
217 increased with Fe loadings due to the availability of a large number of active sites and because of  
218 right interaction in metal and support. The highest conversions were attained by 60%Fe/ $\text{Al}_2\text{O}_3$ .

219 Co-based catalysts are also the area of several studies for optimization of TCD of natural gas into  
220 H<sub>2</sub> and elemental carbon. The formation of cobalt oxide, i.e. Co<sub>3</sub>O<sub>4</sub> is the main reason for its  
221 superior activity and stability of the catalyst [42]. It is also reported that the higher loading of Co  
222 produces large CNF having bigger diameter due to the agglomeration of the particles [43]. Besides  
223 the excellent performance of Co-based catalysts, its toxicity issues and higher cost as compared to  
224 Ni restricts its usage in both industrial and domestic level [31].  
225 The detailed performance analysis along with reaction conditions of some of the monometallic  
226 catalysts has been summarized in Table 1. Moreover, the catalyst synthesis techniques and carbon  
227 yield have also been presented.

Table 1: Catalytic activity and stability of various monometallic catalyst having different supporters and reaction conditions in fixed bed reactor (FBR) for TCD

S. No	Metal	Support	<sup>(a)</sup> W <sub>c</sub> (g)	Preparation	S.A m <sup>2</sup> g <sup>-1</sup>	<sup>(d)</sup> T <sub>R</sub> (K)	<sup>(e)</sup> R <sub>T</sub> (h)	Conversion/Yield (%)	Carbon	Ref
1.	10%Ni	Al <sub>2</sub> O <sub>3</sub>	0.05	I.M <sup>(c)</sup>	141	853	1	<sup>(g)</sup> 21	-	[34]
2.	10%Ni	MgAl <sub>2</sub> O <sub>4</sub>	0.05	I.M <sup>(c)</sup>	134	853	1	<sup>(g)</sup> 12	-	[34]
3.	10%Ni	MgO	0.05	I.M <sup>(c)</sup>	90	853	1	<sup>(g)</sup> 13	-	[34]
4.	14%Fe	CeO <sub>2</sub>	0.15	C.P <sup>(N)</sup>	11.7	1023	4	<sup>(g)</sup> 03	-	[44]
5.	28%Fe	CeO <sub>2</sub>	0.15	C.P <sup>(N)</sup>	22.2	1023	4	<sup>(g)</sup> 05	-	[44]
6.	42%Fe	CeO <sub>2</sub>	0.15	C.P <sup>(N)</sup>	51.3	1023	4	<sup>(g)</sup> 26	-	[44]
7.	56%Fe	CeO <sub>2</sub>	0.15	C.P <sup>(N)</sup>	60.3	1023	4	<sup>(g)</sup> 25	-	[44]
8.	70%Fe	CeO <sub>2</sub>	0.15	C.P <sup>(N)</sup>	69.5	1023	4	<sup>(g)</sup> 10	-	[44]
9.	00%Fe	CeO <sub>2</sub>	0.15	C.P <sup>(N)</sup>	100.2	1023	4	<sup>(g)</sup> 01	-	[44]
10.	67%Fe	Al <sub>2</sub> O <sub>3</sub>	0.15	I.M <sup>(c)</sup>	141.6	1073	3	<sup>(f)</sup> 28	-	[39]
11.	67%Fe	MgO	0.15	I.M <sup>(c)</sup>	14.7	1073	3	<sup>(f)</sup> 20	-	[39]
12.	05%Ni	Al <sub>2</sub> O <sub>3</sub>	0.15	I.M <sup>(c)</sup>	249	973	4	<sup>(g)</sup> 10	-	[32]
13.	7.5%Ni	Al <sub>2</sub> O <sub>3</sub>	0.15	I.M <sup>(c)</sup>	248	973	4	<sup>(g)</sup> 18	-	[32]
14.	10%Ni	Al <sub>2</sub> O <sub>3</sub>	0.15	I.M <sup>(c)</sup>	245	973	4	<sup>(g)</sup> 29	-	[32]
15.	50%Co	MgO	0.5	I.M <sup>(c)</sup>	20.4	973	7	<sup>(g)</sup> 83	<sup>(i)</sup> 261	[45]
16.	50%Fe	MgO	0.5	I.M <sup>(c)</sup>	18.68	973	8	<sup>(f)</sup> 40	<sup>(i)</sup> 599	[46]
17.	50%Ni	MgO	0.5	I.M <sup>(c)</sup>	28.12	973	8	<sup>(f)</sup> 15	<sup>(i)</sup> 139	[46]
18.	50%Co	MgO	0.5	I.M <sup>(c)</sup>	28.25	973	8	<sup>(f)</sup> 90	<sup>(i)</sup> 1121	[46]

S. No	Metal	Support	<sup>(a)</sup> Wc (g)	Preparation	S.A m <sup>2</sup> g <sup>-1</sup>	<sup>(d)</sup> T <sub>R</sub> (K)	<sup>(e)</sup> R <sub>T</sub> (h)	Conversion/Yield (%)	Carbon	Ref
20.	Ni	SiO <sub>2</sub>	3	S.G <sup>(O)</sup>	-	1073	5	<sup>(f)</sup> 50	<sup>(i)</sup> 215	[47]
19.	Co	SiO <sub>2</sub>	3	S.G <sup>(O)</sup>	-	1073	5	<sup>(f)</sup> 47	<sup>(i)</sup> 156	[47]
21.	Fe	SiO <sub>2</sub>	3	S.G <sup>(O)</sup>	-	1073	5	<sup>(f)</sup> 48	<sup>(i)</sup> 177	[47]
22.	15%Fe	SiO <sub>2</sub>	0.3	I.M <sup>(c)</sup>	179.3	973	4	<sup>(f)</sup> 4	-	[28]
23.	25%Fe	SiO <sub>2</sub>	0.3	I.M <sup>(c)</sup>	141	973	4	<sup>(f)</sup> 12	-	[28]
24.	35%Fe	SiO <sub>2</sub>	0.3	I.M <sup>(c)</sup>	135	973	4	<sup>(f)</sup> 15	-	[28]
25.	40%Fe	SiO <sub>2</sub>	0.3	I.M <sup>(c)</sup>	129.5	973	4	<sup>(f)</sup> 54	-	[28]
26.	60%Fe	SiO <sub>2</sub>	0.3	I.M <sup>(c)</sup>	112.6	973	4	<sup>(f)</sup> 71	-	[28]
27.	80%Fe	SiO <sub>2</sub>	0.3	I.M <sup>(c)</sup>	51.9	973	4	<sup>(f)</sup> 74	-	[28]
28.	100%Fe	SiO <sub>2</sub>	0.3	I.M <sup>(c)</sup>	5.4	973	4	<sup>(f)</sup> 78	-	[28]
29.	50%Ni	MgO	0.5	I.M <sup>(c)</sup>	-	973	7	<sup>(f)</sup> 14	-	[48]
30.	10%Fe	Al <sub>2</sub> O <sub>3</sub>	0.3	I.M <sup>(c)</sup>	222.5	973	3	<sup>(g)</sup> 9	-	[40]
31.	20%Fe	Al <sub>2</sub> O <sub>3</sub>	0.3	I.M <sup>(c)</sup>	237	973	3	<sup>(g)</sup> 35	-	[40]
32.	30%Fe	Al <sub>2</sub> O <sub>3</sub>	0.3	I.M <sup>(c)</sup>	203	973	3	<sup>(g)</sup> 42	-	[40]
33.	40%Fe	Al <sub>2</sub> O <sub>3</sub>	0.3	I.M <sup>(c)</sup>	184.8	973	3	<sup>(g)</sup> 43	-	[40]
34.	50%Fe	Al <sub>2</sub> O <sub>3</sub>	0.3	I.M <sup>(c)</sup>	176.2	973	3	<sup>(g)</sup> 45	-	[40]
35.	10%Fe	MgO	0.3	I.M <sup>(c)</sup>	125.1	973	3	<sup>(g)</sup> 44	-	[40]
36.	15%Fe	MgO	0.3	I.M <sup>(c)</sup>	120.8	973	3	<sup>(g)</sup> 47	-	[40]
37.	20%Fe	MgO	0.3	I.M <sup>(c)</sup>	105.8	973	3	<sup>(g)</sup> 46	-	[40]

S. No	Metal	Support	<sup>(a)</sup> Wc (g)	Preparation	S.A m <sup>2</sup> g <sup>-1</sup>	<sup>(d)</sup> T <sub>R</sub> (K)	<sup>(e)</sup> R <sub>T</sub> (h)	Conversion/Yield (%)	Carbon	Ref
38.	30%Fe	MgO	0.3	I.M <sup>(c)</sup>	97.2	973	3	<sup>(g)</sup> 45	-	[40]
39.	40%Fe	MgO	0.3	I.M <sup>(c)</sup>	46.9	973	3	<sup>(g)</sup> 40	-	[40]
40.	20%Fe	TiO <sub>2</sub>	0.3	I.M <sup>(c)</sup>	96.2	973	3	<sup>(g)</sup> 14	-	[40]
41.	30%Fe	TiO <sub>2</sub>	0.3	I.M <sup>(c)</sup>	92	973	3	<sup>(g)</sup> 15	-	[40]
42.	40%Fe	TiO <sub>2</sub>	0.3	I.M <sup>(c)</sup>	76	973	3	<sup>(g)</sup> 16	-	[40]
43.	50%Fe	TiO <sub>2</sub>	0.3	I.M <sup>(c)</sup>	75.9	973	3	<sup>(g)</sup> 17	-	[40]
44.	50%Ni	SBA-15	1	I.M <sup>(c)</sup>	182.6	973	7	<sup>(f)</sup> 40	-	[49]
45.	Ni	MgAl <sub>2</sub> O <sub>4</sub>	1	-	22.63	973	7	<sup>(f)</sup> 34	-	[50]
46.	50%Co	Al <sub>2</sub> O <sub>3</sub>	0.5	I.M <sup>(c)</sup>	24.2	973	7	<sup>(f)</sup> 88	<sup>(i)</sup> 298	[51]
47.	50%Co	SiO <sub>2</sub>	0.5	I.M <sup>(c)</sup>	93.2	973	7	<sup>(f)</sup> 48	<sup>(i)</sup> 172	[51]
48.	50%Co	MgO	0.5	I.M <sup>(c)</sup>	20.1	973	7	<sup>(f)</sup> 73	<sup>(i)</sup> 1121	[51]
49.	30%Ni	Al <sub>2</sub> O <sub>3</sub>	0.05	I.M <sup>(c)</sup>	121.3	973	5	-	-	[31]
50.	40%Ni	Al <sub>2</sub> O <sub>3</sub>	0.05	I.M <sup>(c)</sup>	105.6	973	5	-	-	[31]
51.	50%Ni	Al <sub>2</sub> O <sub>3</sub>	0.05	I.M <sup>(c)</sup>	89.2	973	5	-	-	[31]
52.	60%Ni	Al <sub>2</sub> O <sub>3</sub>	0.05	I.M <sup>(c)</sup>	66.1	973	5	-	-	[31]
53.	60%Ni (N.P) <sup>(K)</sup>	Al <sub>2</sub> O <sub>3</sub>	0.5	-	58.7	973	6	<sup>(f)</sup> 60	-	[33]
54.	60%Ni (B) <sup>(L)</sup>	Al <sub>2</sub> O <sub>3</sub>	0.5	-	22.8	973	6	<sup>(f)</sup> 50	-	[33]
55.	60%Ni (H.S) <sup>(M)</sup>	Al <sub>2</sub> O <sub>3</sub>	0.5	-	22.0	973	6	<sup>(f)</sup> 19	-	[33]
56.	5%Co	SiO <sub>2</sub>	-	I.M <sup>(c)</sup>	382	-	3	-	-	[52]
57.	10%Co	SiO <sub>2</sub>	-	I.M <sup>(c)</sup>	351	-	3	-	-	[52]

S. No	Metal	Support	<sup>(a)</sup> W <sub>c</sub> (g)	Preparation	S.A m <sup>2</sup> g <sup>-1</sup>	<sup>(d)</sup> T <sub>R</sub> (K)	<sup>(e)</sup> R <sub>T</sub> (h)	Conversion/Yield (%)	Carbon	Ref
58.	20%Co	SiO <sub>2</sub>	-	I.M <sup>(c)</sup>	292	-	3	-	-	[52]
59.	5%Co	Al <sub>2</sub> O <sub>3</sub>	-	I.M <sup>(c)</sup>	227	-	3	-	-	[52]
60.	10%Co	Al <sub>2</sub> O <sub>3</sub>	-	I.M <sup>(c)</sup>	27.4	-	3	-	-	[52]
61.	30%Fe	Al <sub>2</sub> O <sub>3</sub>	0.3	I.M <sup>(c)</sup>	150.1	973	3	<sup>(g)</sup> 68	-	[53]
62.	-	NiO	2	-	25.4	1073	6	<sup>(f)</sup> 62	<sup>(i)</sup> 263	[54]
63.	-	Fe <sub>2</sub> O <sub>3</sub>	2	-	13.8	1073	6	<sup>(f)</sup> 50	<sup>(i)</sup> 147	[54]
64.	20%Ni	CeO <sub>2</sub>	2	-	42.1	973	6	<sup>(f)</sup> 62	<sup>(i)</sup> 1360	[35]
65.	20%Ni	ZrO <sub>2</sub>	2	-	23.8	973	6	<sup>(f)</sup> 61	<sup>(i)</sup> 1159	[35]
66.	20%Ni	La <sub>2</sub> O <sub>3</sub>	2	-	10.6	973	6	<sup>(f)</sup> 68	<sup>(i)</sup> 1576	[35]
67.	Ni	Al <sub>2</sub> O <sub>3</sub>	-	I.M <sup>(c)</sup>	201.03	1073	4	<sup>(g)</sup> 15.33	-	[55]
68.	Pd	Al <sub>2</sub> O <sub>3</sub>	-	I.M <sup>(c)</sup>	195.31	1073	4	<sup>(g)</sup> 15.68	-	[55]
69.	10%Ni	TiO <sub>2</sub>	1	I.M <sup>(c)</sup>	23.68	973	6	<sup>(f)</sup> 27	<sup>(i)</sup> 1399	[37]
70.	20%Ni	TiO <sub>2</sub>	1	I.M <sup>(c)</sup>	18.49	973	6	<sup>(f)</sup> 30	<sup>(i)</sup> 1180	[37]
71.	30%Ni	TiO <sub>2</sub>	1	I.M <sup>(c)</sup>	12.31	973	6	<sup>(f)</sup> 33	<sup>(i)</sup> 1380	[37]
72.	40%Ni	TiO <sub>2</sub>	1	I.M <sup>(c)</sup>	-	973	6	<sup>(f)</sup> 37	<sup>(i)</sup> 1522	[37]
73.	50%Ni	TiO <sub>2</sub>	1	I.M <sup>(c)</sup>	-	973	6	<sup>(f)</sup> 42	<sup>(i)</sup> 1544	[37]
74.	Ni	MgO	1	I.M <sup>(c)</sup>	24.20	1073	6	<sup>(f)</sup> 37	<sup>(i)</sup> 850	[56]
75.	5%Fe	MgO	0.5	I.M <sup>(c)</sup>	79	1173	-	-	<sup>(i)</sup> 4.7	[57]

(a)Weight of catalyst (b) Fusion method (c) Impregnation method (d) Reaction temperature (e) Reaction Time (f) H<sub>2</sub> yield (g) Methane (h) g c/ g ni

(i) % (J) mg (K) Nano particle (L) Bulk (M) Hollow Sphere (N) Co Precipitation (O) Sol Gel

## 2.2. Bi-Metallic Catalyst

The transition metals such as Ni, Fe, and Co as explained in [Section 2.1](#) have shown better performance as active metal precursors for TCD of CH<sub>4</sub> into CO<sub>x</sub> free H<sub>2</sub> and CNF [58]. The deactivation of this catalyst at high temperatures is due to the encapsulation of nearly in active carbon. This has opened new horizons of research in this field (c.f. Table 1). The modification of Ni-based catalyst with other transition metals is reported to be a viable solution to this problem [59]. The impregnation of a second metal on Ni provides significant changes in its activity and stability due to alloying effect [45] (c.f. Tables 2 and 3).

To optimize the TCD of CH<sub>4</sub>, innumerable Ni-based bimetallic catalysts supported on  $\gamma$ -Al<sub>2</sub>O<sub>3</sub> were employed. It was reported that Ni acts as an active phase and Al<sub>2</sub>O<sub>3</sub> being inactive, which aids the dispersion of Ni-containing phases. Interestingly, inactive Al<sub>2</sub>O<sub>3</sub> proved to be responsible for most of the mechanical properties exhibited by the catalyst [60]. Echegoyen et al. [61] reported that the addition of textural promoter in Ni-based catalyst prevent from sintering. The group synthesized Cu promoted catalyst supported on MgO. The presence of Cu enhanced the catalytic stability of the catalyst for 8 h. Cu itself is inactive for TCD of CH<sub>4</sub>. The basic function is to aid CNF formation and increase the carbon diffusion rate, thus keeping the surface of Ni fresh for CH<sub>4</sub> adsorption. Moreover, Cu promoted catalyst results in the formation of broader and lengthier CNF as a by-product [62]. A further study from [63] concluded that TiO<sub>2</sub> could also use as textural support on high loading bimetallic catalyst and presence of Cu as promoter either in the form of oxide or nitrate enhance conversions of CH<sub>4</sub> and carbon formations.

The influence of Mo on the catalytic efficiency of Ni/Al<sub>2</sub>O<sub>3</sub> was investigated in [64]. The results showed that addition of Mo with other transition metals improves CH<sub>4</sub> conversions and CNT production as carbon bundles. Another critical aspect of Mo is its reduction to molybdenum

carbides at the initial stages of the reaction. Ni and Mo both serve TCD of CH<sub>4</sub> and CNT formation in different ways. The former is responsible for the dissociation of CH<sub>4</sub> into H<sub>2</sub> and elemental carbon while the latter serves as a reservoir for carbon diffusion. The presence of Mo as a promoter impregnated on Al<sub>2</sub>O<sub>3</sub> in Ni-based catalysts provided strong MSI and minimized sintering of material and ultimately increase the catalytic stability [65]. It was also observed in the above study that TCD of CH<sub>4</sub> is not affected by the surface measurements of the catalyst [65].

Awadallah et al. [43] studied the effects of Co loadings on Mo/Al<sub>2</sub>O<sub>3</sub>. The results summarized that CH<sub>4</sub> conversions and diameter of CNF increased intermittently with higher metal loadings despite the decline in surface area which confirmed that TCD is a metal-catalyzed reaction. The presence of ample amount of Co<sub>3</sub>O<sub>4</sub> on the surface of the catalyst boosted the catalyst stability. The transition metals of group VI (Mo, Cr, W) were impregnated with Co/MgO [45]. The results revealed that the CH<sub>4</sub> decompositions were stable for longer runs due to the formation of mixed oxides, i.e. CoMoO<sub>4</sub> and CoWO<sub>4</sub> which increased the dispersion and stabilization of Co particles. The carbon yield exhibited was in the order of Mo > W > Cr. Bimetallic metals of group VIII Ni, Fe and Co supported on MgO with a total metal content of 50%. They were tested for non-oxidative decomposition of CH<sub>4</sub> [48]. Fe–Co/MgO achieved the highest catalytic stability due to the presence of Fe<sub>2</sub>O<sub>3</sub> and Co<sub>3</sub>O<sub>4</sub> on the surface of MgO resulting in higher adsorption and solubility of CH<sub>4</sub>. Besides these results, the CH<sub>4</sub> decompositions declined for Ni–Fe and Ni–Co based catalyst due to the formation on stable, robust solution Mg<sub>x</sub>Ni<sub>(1-x)</sub>O. The authors believed that it was difficult to remove Ni species from inactive Mg<sub>x</sub>Ni<sub>(1-x)</sub>O because of powerful MSI. Additionally, RAMAN revealed that the degree of graphitization and crystallinity was high in Fe–Co/MgO as compared to the Ni-based catalyst.

Reasonable results were reported elsewhere [42] as CH<sub>4</sub> conversions increased with higher loadings of cobalt in Co–W/MgO. Presence of large quantities of Co on the surface of the MgO was the primary reason for substantial diffusion of feedstock. Ahmad et al. [66] highlighted the effects of varying the composition of catalyst support on 50% Ni-based catalyst. Different compositions of CeO<sub>2</sub> and Al<sub>2</sub>O<sub>3</sub> as catalyst supporters were synthesized by co-precipitation method and later were impregnated with 50%Ni. The conversions of CH<sub>4</sub> are strongly dependent on the amount of CeO<sub>2</sub> in the catalyst while it also affected the surface properties. The addition of CeO<sub>2</sub> to Al<sub>2</sub>O<sub>3</sub> avoided the formation of inactive NiAl<sub>2</sub>O<sub>4</sub> as confirmed by TPR analysis.

Apart from Ni, numerous works have been done on investigating the stability and activity of the Fe-based catalyst. Al-Fatesh et al. [67] studied the effects of modifying Fe/MgO catalyst by Ni, Co and Mn additives. Both CH<sub>4</sub> conversions and H<sub>2</sub> yields were enhanced in the presence of metal additives in the order of Ni > Co > Mn. It is believed that the catalytic activity is rational to the surface area of the catalyst. However, the authors observed that the activities are dependent on the interaction between metal additives and the availability of active sites. Some other similar studies were also given elsewhere [65].

Ahmad et al. [68] worked on Ce and Co-based Fe/Al<sub>2</sub>O<sub>3</sub>. It was concluded that the catalyst reduced at higher temperature showed a decline in performance due to the sintering of the active sites. Furthermore, the addition of Co and Ce in the bimetallic catalyst provides two types of active sites thus favoring the reaction yields. Additionally, the conversions increased with higher Co loadings [29]. So, it was found that 15% Co coupled with 30%Fe/Al<sub>2</sub>O<sub>3</sub> holds appropriate MSI and metal dispersion that leads to the excellent performance of the catalyst [53]. In another different study compositions of Ni, Co over Al<sub>2</sub>O<sub>3</sub> was studied for TCD of CH<sub>4</sub>. The best results were produced

by using 25% each of Ni and Co (25%NiCoAl). The presence of Co-leads in the formation of thick wall highly stable MWCNT [69].

The same group of scholars [70] studied the effect of preparation method and calcination temperature on the catalytic stability of Ni-Fe/Al<sub>2</sub>O<sub>3</sub>. The results depicted that the CH<sub>4</sub> conversions and carbon morphology is dependent on metal additives, synthesis procedure, and calcination temperatures. The impregnation method gave the highest yields as compared to co-precipitation and sol-gel method irrespective of the calcination temperatures. It was also noticeable that XRD analysis at higher calcination temperatures detected additional peaks of metal aluminates. Wasim et al. [71, 72] employed La<sub>2</sub>O<sub>3</sub> as catalyst support for Ni-Co catalyst. 12.5% of Ni and Co were found to be the optimum composition of the catalyst. The conversions were directly proportional to the reaction temperature owing to the endothermic nature of the reaction while declined with the rise in GHSV. The authors reported CDM as a four-step mechanism which included breakage of CH<sub>4</sub> bonds, the release of H<sub>2</sub>, carbon diffusion and formation and accumulation of CNF over the surface of the catalyst. Moreover, the rise in calcination temperatures also affected the catalytic performance due to the destruction of active sites of the catalyst.

The study on optimizing TCD of CH<sub>4</sub> over bimetallic catalyst was carried on by Bayat et al. [73] with different catalyst compositions and metal additives. The authors impregnated Cu with Ni/Al<sub>2</sub>O<sub>3</sub>. The study revealed that the addition of Cu as promoter enhance TCD in several ways including high metal dispersion, reducibility, and rates of CH<sub>4</sub> adsorption. Moreover, the high affinity of Cu with graphene inhibits the formation of encapsulating carbon and keeps the Ni surface fresh for CH<sub>4</sub> diffusions [74]. This observation was also seen in the study made by Kumar et al. [75]. The successful impregnation of Ni and Cu on Al<sub>2</sub>O<sub>3</sub> synthesized formerly by sol-gel

method resulted in the formation of mixed oxides  $\text{Ni}_x \text{Cu}_{(1-x)} \text{O}$  species and Ni–Cu alloy in the calcined and reduced catalyst. Along with Cu, Pd is also regarded as a strong promoter in catalytic decomposition of  $\text{CH}_4$  into  $\text{CO}_x$  free  $\text{H}_2$  and CNF. Improved catalytic activity and thermal stability are the results of impregnating Pd on Ni-based catalysts [55]. Bayat et al. [76] suggested that the rate of carbon diffusion in Pd is faster as compared to Ni. This aspect results in increasing the diffusion rate of carbon inhibits the formation of encapsulating carbon over Ni. Additionally, during CDM reaction carbon grows from several facets of Ni–Pd alloy forming branched carbon that boosts up catalyst stability and activity. Supportive results were elaborated by the same group in which the authors impregnated Fe on  $\text{Ni}/\text{Al}_2\text{O}_3$  [77]. The addition of Fe improved the conversions at higher temperatures due to its high ability to diffuse carbon thus avoiding the formation of encapsulating carbon. It is also reported that though Fe based catalyst results in fewer conversions as compared to Ni-based. Since the diffusion rate of carbon in the former catalyst is much higher compared to the later one [78]. Many studies have been devoted to modifying the supports by co-precipitating a couple of oxides together. Ahmad et al. [66] synthesized  $\text{CeO}_2\text{--Al}_2\text{O}_3$  as a catalyst support and demonstrated that the conversion of  $\text{CH}_4$  was mostly dependent on  $\text{CeO}_2$  content. In another work by Rastegarpanah et al. [79, 80], it was concluded that  $\text{MgO--Al}_2\text{O}_3$  performed well under a specified set of conditions. The effects of  $\text{TiO}_2\text{--Al}_2\text{O}_3$  were also reported by [38]. The catalytic activity and stability of various catalyst having different supporters and reaction conditions in FBR in TCD for bimetallic catalyst have been furnished in Table 2.

Table 2: Catalytic activity and stability of various catalysts having different supporters and reaction conditions in FBR in TCD

S. No	Metal	Support	<sup>(a)</sup> W <sub>c</sub> (g)	Preparation	S.A m <sup>2</sup> g <sup>-1</sup>	<sup>(d)</sup> T <sub>R</sub> (K)	<sup>(e)</sup> R <sub>T</sub> (h)	Conversion/Yield (%)	Carbon	Ref
1.	Ni-Cu	Al	0.3	F.M <sup>(b)</sup>	-	973	8	<sup>(f)</sup> 75	-	[60]
2.	Ni-Cu	Mg	0.3	F.M <sup>(b)</sup>	-	1073	8	<sup>(f)</sup> 79	-	[61]
3.	Ni-Cu	SiO <sub>2</sub>	0.3	F.M <sup>(b)</sup>	-	1073	8	<sup>(f)</sup> 79	-	[62]
4.	Ni-Cu	TiO <sub>2</sub>	0.3	F.M <sup>(b)</sup>	-	1073	8	<sup>(f)</sup> 80	-	[63]
5.	50%Fe-5%Mo	Al <sub>2</sub> O <sub>3</sub>	0.15	I.M <sup>(c)</sup>	193	1073	3	<sup>(f)</sup> 16	<sup>(h)</sup> 5.9	[39]
6.	50%Fe-7.5%Mo	MgO	0.15	I.M <sup>(c)</sup>	15.3	1073	3	<sup>(f)</sup> 28	<sup>(h)</sup> 4.75	[39]
7.	Ni-Cu	MgO	0.2	I.M <sup>(c)</sup>	-	843	4	<sup>(f)</sup> 58	<sup>(h)</sup> 5.85	[81]
8.	Ni-Mo	MgO	0.2	I.M <sup>(c)</sup>	-	843	4	<sup>(f)</sup> 15	<sup>(h)</sup> 3.90	[81]
9.	Ni-Co	MgO	0.2	I.M <sup>(c)</sup>	-	843	4	<sup>(f)</sup> 14	-	[81]
10.	Ni-Mo	Al <sub>2</sub> O <sub>3</sub>	0.5	I.M <sup>(c)</sup>	-	1073	8	-	<sup>(i)</sup> 669	[64]
11.	5.2%Ni-10.96%Mo	Al <sub>2</sub> O <sub>3</sub>	0.5	I.M <sup>(c)</sup>	127.9	973	8	<sup>(f)</sup> 70	<sup>(i)</sup> 341	[65]
12.	10%Ni-9.5%Mo	Al <sub>2</sub> O <sub>3</sub>	0.5	I.M <sup>(c)</sup>	101.2	973	8	<sup>(f)</sup> 80	<sup>(i)</sup> 612	[65]
13.	20%Ni-8.5%Mo	Al <sub>2</sub> O <sub>3</sub>	0.5	I.M <sup>(c)</sup>	89.2	973	8	<sup>(f)</sup> 81	<sup>(i)</sup> 834	[65]
14.	30%Ni-7.5%Mo	Al <sub>2</sub> O <sub>3</sub>	0.5	I.M <sup>(c)</sup>	91.3	973	8	<sup>(f)</sup> 82	<sup>(i)</sup> 1009	[65]
15.	40%Ni-6.5%Mo	Al <sub>2</sub> O <sub>3</sub>	0.5	I.M <sup>(c)</sup>	71.4	973	8	<sup>(f)</sup> 82	<sup>(i)</sup> 1379	[65]
16.	3.1%Co-10.5%Mo	Al <sub>2</sub> O <sub>3</sub>	0.5	I.M <sup>(c)</sup>	190.9	973	8	<sup>(f)</sup> 15	<sup>(i)</sup> 55	[43]
17.	10%Co-9.3%Mo	Al <sub>2</sub> O <sub>3</sub>	0.5	I.M <sup>(c)</sup>	177.4	973	8	<sup>(f)</sup> 65	<sup>(i)</sup> 762	[43]

S. No	Metal	Support	<sup>(a)</sup> W <sub>c</sub> (g)	Preparation	S.A m <sup>2</sup> g <sup>-1</sup>	<sup>(d)</sup> T <sub>R</sub> (K)	<sup>(e)</sup> R <sub>T</sub> (h)	Conversion/Yield (%)	Carbon	Ref
18.	20%Co–8.3%Mo	Al <sub>2</sub> O <sub>3</sub>	0.5	I.M <sup>(c)</sup>	143.9	973	8	<sup>(f)</sup> 82	<sup>(i)</sup> 456	[43]
19.	30%Co–7.3%Mo	Al <sub>2</sub> O <sub>3</sub>	0.5	I.M <sup>(c)</sup>	124.8	973	8	<sup>(f)</sup> 83	<sup>(i)</sup> 517	[43]
20.	40%Co–6.3%Mo	Al <sub>2</sub> O <sub>3</sub>	0.5	I.M <sup>(c)</sup>	107.6	973	8	<sup>(f)</sup> 84	<sup>(i)</sup> 568	[43]
21.	20%Ni–20%Co	Al <sub>2</sub> O <sub>3</sub>	0.3	I.M <sup>(c)</sup>	151	973	5	<sup>(g)</sup> 70	<sup>(i)</sup> 600	[69]
22.	22%Ni–22%Co	Al <sub>2</sub> O <sub>3</sub>	0.3	I.M <sup>(c)</sup>	150	973	5	<sup>(g)</sup> 72	<sup>(i)</sup> 700	[69]
23.	25%Ni–25%Co	Al <sub>2</sub> O <sub>3</sub>	0.3	I.M <sup>(c)</sup>	120	973	5	<sup>(g)</sup> 74	<sup>(i)</sup> 850	[69]
24.	27%Ni–27%Co	Al <sub>2</sub> O <sub>3</sub>	0.3	I.M <sup>(c)</sup>	123	973	5	<sup>(g)</sup> 73	<sup>(i)</sup> 720	[69]
25.	30%Ni–30%Co	Al <sub>2</sub> O <sub>3</sub>	0.3	I.M <sup>(c)</sup>	127	973	5	<sup>(g)</sup> 70	<sup>(i)</sup> 650	[69]
26.	25%Co–25%Cr	MgO	0.5	I.M <sup>(c)</sup>	39.8	973	7	<sup>(g)</sup> 73	<sup>(h)</sup> 1.6	[45]
27.	25%Co–25%Mo	MgO	0.5	I.M <sup>(c)</sup>	50.7	973	7	<sup>(g)</sup> 81	<sup>(h)</sup> 2.38	[45]
28.	25%Co–25%W	MgO	0.5	I.M <sup>(c)</sup>	34.5	973	7	<sup>(g)</sup> 76	<sup>(h)</sup> 2.04	[45]
29.	40%Co–10%W	MgO	0.5	I.M <sup>(c)</sup>	38.1	973	7	<sup>(g)</sup> 85	<sup>(i)</sup> 280	[42]
30.	30%Co–20%W	MgO	0.5	I.M <sup>(c)</sup>	36.8	973	7	<sup>(g)</sup> 73	<sup>(i)</sup> 237	[42]
31.	20%Co–30%W	MgO	0.5	I.M <sup>(c)</sup>	29.5	973	7	<sup>(g)</sup> 69	<sup>(i)</sup> 229	[42]
32.	10%Co–40%W	MgO	0.5	I.M <sup>(c)</sup>	16.7	973	7	<sup>(g)</sup> 20	<sup>(i)</sup> 51	[42]
33.	25%Fe–25%Co	MgO	0.5	I.M <sup>(c)</sup>	52.7	973	7	<sup>(f)</sup> 82	<sup>(i)</sup> 340	[48]
34.	25%Ni–25%Fe	MgO	0.5	I.M <sup>(c)</sup>	68.2	973	7	<sup>(f)</sup> 16	<sup>(i)</sup> 411	[48]
35.	25%Ni–25%Co	MgO	0.5	I.M <sup>(c)</sup>	24.1	973	7	<sup>(f)</sup> 13	<sup>(i)</sup> 766	[48]

S. No	Metal	Support	<sup>(a)</sup> W <sub>c</sub> (g)	Preparation	S.A m <sup>2</sup> g <sup>-1</sup>	<sup>(d)</sup> T <sub>R</sub> (K)	<sup>(e)</sup> R <sub>T</sub> (h)	Conversion/Yield (%)	Carbon	Ref
36.	60%Ni	15%TiO <sub>2</sub> -Al <sub>2</sub> O <sub>3</sub>	0.5	I.M <sup>(c)</sup>	94	973	7	<sup>(f)</sup> 25	<sup>(i)</sup> 126	[38]
37.	60%Ni	25%TiO <sub>2</sub> -Al <sub>2</sub> O <sub>3</sub>	0.5	I.M <sup>(c)</sup>	135	973	7	<sup>(f)</sup> 60	<sup>(i)</sup> 504	[38]
38.	60%Ni	50%TiO <sub>2</sub> -Al <sub>2</sub> O <sub>3</sub>	0.5	I.M <sup>(c)</sup>	70	973	7	<sup>(f)</sup> 65	<sup>(i)</sup> 413	[38]
39.	Ni-Pd	MgAl <sub>2</sub> O <sub>4</sub>	1	-	29.38	973	5	<sup>(f)</sup> 43	-	[50]
40.	Ni-Co	SBA-15	3	I.M <sup>(c)</sup>	312.0	973	5	<sup>(f)</sup> 44	<sup>(i)</sup> 257	[47]
41.	Ni-Fe	SBA-15	3	I.M <sup>(c)</sup>	294.0	973	5	<sup>(f)</sup> 41	<sup>(i)</sup> 233	[47]
42.	Co-Fe	SBA-15	3	I.M <sup>(c)</sup>	286.0	973	5	<sup>(f)</sup> 46	<sup>(i)</sup> 233	[47]
43.	50%Ni-0.2%Pd	SBA-15	1	I.M <sup>(c)</sup>	198.2	973	7	<sup>(f)</sup> 45	<sup>(i)</sup> 489	[49]
44.	50%Ni-0.4%Pd	SBA-15	1	I.M <sup>(c)</sup>	201.8	973	7	<sup>(f)</sup> 50	<sup>(i)</sup> 489	[49]
45.	12.5%Ni-12.5%Co	La <sub>2</sub> O <sub>3</sub>	0.3	I.M <sup>(c)</sup>	63.3	973	5	<sup>(f)</sup> 77	-	[72]
46.	50%Ni-5%Fe	Al <sub>2</sub> O <sub>3</sub>	0.05	I.M <sup>(c)</sup>	83.7	948	11	<sup>(g)</sup> 35	-	[77]
47.	50%Ni-10%Fe	Al <sub>2</sub> O <sub>3</sub>	0.05	I.M <sup>(c)</sup>	78.8	948	11	<sup>(g)</sup> 70	-	[77]
48.	50%Ni-15%Fe	Al <sub>2</sub> O <sub>3</sub>	0.05	I.M <sup>(c)</sup>	74.8	948	11	<sup>(g)</sup> 68	-	[77]
49.	7.39%Ni-7.28%Co	La <sub>2</sub> O <sub>3</sub>	0.3	I.M <sup>(c)</sup>	30.19	973	5	<sup>(g)</sup> 70	<sup>(i)</sup> 20	[71]
50.	9.81%Ni-9.72%Co	La <sub>2</sub> O <sub>3</sub>	0.3	I.M <sup>(c)</sup>	61.64	973	5	<sup>(g)</sup> 79	<sup>(i)</sup> 50	[71]
51.	11.32%Ni-12.11%Co	La <sub>2</sub> O <sub>3</sub>	0.3	I.M <sup>(c)</sup>	63.32	973	5	<sup>(g)</sup> 80	<sup>(i)</sup> 90	[71]
52.	14.75%Ni-13.92%Co	La <sub>2</sub> O <sub>3</sub>	0.3	I.M <sup>(c)</sup>	56.02	973	5	<sup>(g)</sup> 79	<sup>(i)</sup> 60	[71]
53.	18.85%Ni-19.63%Co	La <sub>2</sub> O <sub>3</sub>	0.3	I.M <sup>(c)</sup>	48.45	973	5	<sup>(g)</sup> 78	<sup>(i)</sup> 35	[71]
54.	Ni-Pd	Al <sub>2</sub> O <sub>3</sub>	-	I.M <sup>(c)</sup>	212.80	1073	4	<sup>(g)</sup> 40	-	[55]
55.	65%Ni-10%Cu	SiO <sub>2</sub>	-	-	37.70	923	6	<sup>(g)</sup> 43	-	[82]

S. No	Metal	Support	<sup>(a)</sup> W <sub>c</sub> (g)	Preparation	S.A m <sup>2</sup> g <sup>-1</sup>	<sup>(d)</sup> T <sub>R</sub> (K)	<sup>(e)</sup> R <sub>T</sub> (h)	Conversion/Yield (%)	Carbon	Ref
56.	50%Ni–20%Cu	SiO <sub>2</sub>	-	-	27.83	923	6	<sup>(g)</sup> 27	-	[82]
57.	5%Ni–Cu	Al <sub>2</sub> O <sub>3</sub>	2.5	I.M <sup>(c)</sup>	63.80	1123	4	<sup>(f)</sup> 40	-	[83]
58.	10%Ni–Cu	Al <sub>2</sub> O <sub>3</sub>	2.5	I.M <sup>(c)</sup>	84.10	1123	4	<sup>(f)</sup> 58	-	[83]
59.	15%Ni–Cu	Al <sub>2</sub> O <sub>3</sub>	2.5	I.M <sup>(c)</sup>	42.60	1123	4	<sup>(f)</sup> 52	-	[83]
60.	20%Ni–Cu	Al <sub>2</sub> O <sub>3</sub>	2.5	I.M <sup>(c)</sup>	34.30	1123	4	<sup>(f)</sup> 37	-	[83]
61.	50%Ni-5%Pd	Al <sub>2</sub> O <sub>3</sub>	0.05	I.M <sup>(c)</sup>	72.75	1023	10	<sup>(g)</sup> 65	<sup>(j)</sup> 360	[76]
62.	50%Ni-10%Pd	Al <sub>2</sub> O <sub>3</sub>	0.05	I.M <sup>(c)</sup>	45.81	1023	10	<sup>(g)</sup> 72	<sup>(j)</sup> 380	[76]
63.	50%Ni-15%Pd	Al <sub>2</sub> O <sub>3</sub>	0.05	I.M <sup>(c)</sup>	26.91	1023	10	<sup>(g)</sup> 81	<sup>(j)</sup> 400	[76]
64.	50%Ni-20%Pd	Al <sub>2</sub> O <sub>3</sub>	0.05	I.M <sup>(c)</sup>	12.36	1023	10	<sup>(g)</sup> 76	<sup>(j)</sup> 410	[76]
65.	30%Fe–6%Ce	Al <sub>2</sub> O <sub>3</sub>	-	I.M <sup>(c)</sup>	56.25	973	3	<sup>(f)</sup> 66	-	[68]
66.	30%Fe–15%Ce	Al <sub>2</sub> O <sub>3</sub>	-	I.M <sup>(c)</sup>	52.1	973	3	<sup>(f)</sup> 62	-	[68]
67.	30%Fe–30%Ce	Al <sub>2</sub> O <sub>3</sub>	-	I.M <sup>(c)</sup>	95.3	973	3	<sup>(f)</sup> 54	-	[68]
68.	50%Ni-5%Cu	Al <sub>2</sub> O <sub>3</sub>	0.05	I.M <sup>(c)</sup>	72.25	1023	11	<sup>(g)</sup> 20	-	[73]
69.	50%Ni-10%Cu	Al <sub>2</sub> O <sub>3</sub>	0.05	I.M <sup>(c)</sup>	70.34	1023	11	<sup>(g)</sup> 79	-	[73]
70.	50%Ni-15%Cu	Al <sub>2</sub> O <sub>3</sub>	0.05	I.M <sup>(c)</sup>	51.89	1023	11	<sup>(g)</sup> 84	-	[73]
71.	30%Fe–15%Ni	Al <sub>2</sub> O <sub>3</sub>	0.3	I.M <sup>(c)</sup>	132.5	973	3	<sup>(g)</sup> 73	-	[53]
72.	30%Fe–15%Co	Al <sub>2</sub> O <sub>3</sub>	0.3	I.M <sup>(c)</sup>	133.6	973	3	<sup>(g)</sup> 74	<sup>(h)</sup> 15	[53]
73.	5%Ni–20%Fe	Al <sub>2</sub> O <sub>3</sub>	0.3	I.M <sup>(c)</sup>	147.7	973	3	<sup>(g)</sup> 65	-	[70]
74.	10%Ni–20%Fe	Al <sub>2</sub> O <sub>3</sub>	0.3	I.M <sup>(c)</sup>	140.6	973	3	<sup>(g)</sup> 66	-	[70]
75.	30%Fe–6%Co	Al <sub>2</sub> O <sub>3</sub>	0.3	I.M <sup>(c)</sup>	43.4	973	3	<sup>(g)</sup> 66	-	[29]

S. No	Metal	Support	<sup>(a)</sup> W <sub>c</sub> (g)	Preparation	S.A m <sup>2</sup> g <sup>-1</sup>	<sup>(d)</sup> T <sub>R</sub> (K)	<sup>(e)</sup> R <sub>T</sub> (h)	Conversion/Yield (%)	Carbon	Ref
76.	30%Fe–15%Co	Al <sub>2</sub> O <sub>3</sub>	0.3	I.M <sup>(c)</sup>	52.4	973	3	<sup>(g)</sup> 74	-	[29]
77.	30%Fe–30%Co	Al <sub>2</sub> O <sub>3</sub>	0.3	I.M <sup>(c)</sup>	72	973	3	<sup>(g)</sup> 71	-	[29]
78.	50%Ni	25%CeO <sub>2</sub> –75% Al <sub>2</sub> O <sub>3</sub>	0.5	I.M <sup>(c)</sup>	34	973	6	<sup>(f)</sup> 52	-	[66]
79.	50%Ni	50%CeO <sub>2</sub> –50% Al <sub>2</sub> O <sub>3</sub>	0.5	I.M <sup>(c)</sup>	51	973	6	<sup>(f)</sup> 40	-	[66]
80.	50%Ni	75%CeO <sub>2</sub> –25% Al <sub>2</sub> O <sub>3</sub>	0.5	I.M <sup>(c)</sup>	69	973	6	<sup>(f)</sup> 42	-	[66]
81.	15%Fe–6%Ni	MgO	0.3	I.M <sup>(c)</sup>	100	973	3	<sup>(g)</sup> 66	<sup>(h)</sup> 16.26	[67]
82.	15%Fe–6%Co	MgO	0.3	I.M <sup>(c)</sup>	86	973	3	<sup>(g)</sup> 69	<sup>(h)</sup> 15.06	[67]
83.	15%Fe–6%Mn	MgO	0.3	I.M <sup>(c)</sup>	122	973	3	<sup>(g)</sup> 68	<sup>(h)</sup> 15.49	[67]
84.	5%Fe–1%Mo	MgO	0.5	I.M <sup>(c)</sup>	90	1173	-	-	<sup>(i)</sup> 32.3	[57]
85.	5%Fe–1%Cu	MgO	0.5	I.M <sup>(c)</sup>	54	1173	-	-	<sup>(i)</sup> 5.8	[57]
86.	50%Ni	SiO <sub>2</sub> – Al <sub>2</sub> O <sub>3</sub>	0.5	I.M <sup>(c)</sup>	107	973	3	<sup>(f)</sup> 60	-	[84]
87.	50%Ni	SiO <sub>2</sub> –CeO <sub>2</sub>	0.5	I.M <sup>(c)</sup>	37	973	3	<sup>(f)</sup> 55	-	[84]
88.	50%Ni	SiO <sub>2</sub> –La <sub>2</sub> O <sub>3</sub>	0.5	I.M <sup>(c)</sup>	44	973	3	<sup>(f)</sup> 58	-	[84]
89.	50%Ni	SiO <sub>2</sub> – MgO	0.5	I.M <sup>(c)</sup>	54	973	3	<sup>(f)</sup> 13	-	[84]
90.	55%Ni	MgO–Al <sub>2</sub> O <sub>3</sub>	0.025	-	66.31	948	5	<sup>(g)</sup> 8	<sup>(j)</sup> 140	[80]
91.	55%Ni–10%Ce	MgO–Al <sub>2</sub> O <sub>3</sub>	0.025	-	55.06	948	5	<sup>(g)</sup> 12	<sup>(j)</sup> 150	[80]
92.	55%Ni–10%Co	MgO–Al <sub>2</sub> O <sub>3</sub>	0.025	-	46.84	948	5	<sup>(g)</sup> 12	<sup>(j)</sup> 120	[80]
93.	55%Ni–10%Cu	MgO–Al <sub>2</sub> O <sub>3</sub>	0.025	-	43.57	948	5	<sup>(g)</sup> 10	<sup>(j)</sup> 280	[80]
94.	55%Ni–10%Fe	MgO–Al <sub>2</sub> O <sub>3</sub>	0.025	-	66.18	948	5	<sup>(g)</sup> 13	<sup>(j)</sup> 100	[80]
95.	55%Ni–10%La	MgO–Al <sub>2</sub> O <sub>3</sub>	0.025	-	41.86	948	5	<sup>(g)</sup> 11	<sup>(j)</sup> 120	[80]

S. No	Metal	Support	<sup>(a)</sup> W <sub>c</sub> (g)	Preparation	S.A m <sup>2</sup> g <sup>-1</sup>	<sup>(d)</sup> T <sub>R</sub> (K)	<sup>(e)</sup> R <sub>T</sub> (h)	Conversion/Yield (%)	Carbon	Ref
96.	10%Ni	0.5%MgO–Al <sub>2</sub> O <sub>3</sub>	0.025	-	236.0	973	5	<sup>(f)</sup> 05	-	[79]
97.	10%Ni	1.0%MgO–Al <sub>2</sub> O <sub>3</sub>	0.025	-	224.0	973	5	<sup>(f)</sup> 06	-	[79]
98.	10%Ni	1.5%MgO–Al <sub>2</sub> O <sub>3</sub>	0.025	-	216.0	973	5	<sup>(f)</sup> 08	-	[79]
99.	10%Ni	2.0%MgO–Al <sub>2</sub> O <sub>3</sub>	0.025	-	220.0	898	5	<sup>(g)</sup> 04	-	[79]
100.	25%Ni	2.0%MgO–Al <sub>2</sub> O <sub>3</sub>	0.025	-	149	898	5	<sup>(g)</sup> 05	-	[79]
101.	40%Ni	2.0%MgO–Al <sub>2</sub> O <sub>3</sub>	0.025	-	105	898	5	<sup>(g)</sup> 13	-	[79]
102.	55%Ni	2.0%MgO–Al <sub>2</sub> O <sub>3</sub>	0.025	-	66	898	5	<sup>(g)</sup> 20	-	[79]
103.	6%Ni-30%Fe	Al <sub>2</sub> O <sub>3</sub>	0.3	I.M <sup>(c)</sup>	135.5	973	3	<sup>(g)</sup> 61	-	[85]
104.	15%Ni-30%Fe	Al <sub>2</sub> O <sub>3</sub>	0.3	I.M <sup>(c)</sup>	132.5	973	3	<sup>(g)</sup> 62	-	[85]
105.	30%Ni-30%Fe	Al <sub>2</sub> O <sub>3</sub>	0.3	I.M <sup>(c)</sup>	130.0	973	3	<sup>(g)</sup> 56	-	[85]
106.	6%Mn-30%Fe	Al <sub>2</sub> O <sub>3</sub>	0.3	I.M <sup>(c)</sup>	143.9	973	3	<sup>(g)</sup> 11	-	[85]
107.	15%Mn-30%Fe	Al <sub>2</sub> O <sub>3</sub>	0.3	I.M <sup>(c)</sup>	131.1	973	3	<sup>(g)</sup> 10	-	[85]
108.	30%Mn-30%Fe	Al <sub>2</sub> O <sub>3</sub>	0.3	I.M <sup>(c)</sup>	123.8	973	3	<sup>(g)</sup> 13	-	[85]

(a)Weight of catalyst (b) Fusion method (c) Impregnation method (d) Reaction temperature (e) Reaction Time (f) H<sub>2</sub> yield (g) Methane (h) g c/ g ni (i) % (J) mg

### 2.3.Tri-metallic Catalyst

Sections 2.1 and 2.2 summarized various contributions relevant to this study. Moreover, the effects of monometallic and bimetallic have been explained in Tables 1 and 2 respectively. Although the CH<sub>4</sub> yields were improved with higher metal loadings and shifting from mono metallic to bimetallic due to alloying effect, some of the scholars tried to further optimize the process by taking into account the effectiveness of commissioning trimetallic catalyst for CO<sub>x</sub> free H<sub>2</sub> production [86, 87].

Kumar et al. [88, 89] synthesized different compositions of Ni–Cu–Zn/MCM 22. The catalytic stability was widely explored over reaction temperature, metal loadings, and GHSV. It was depicted that the combination of Cu and Zn enhanced the CH<sub>4</sub> conversions and H<sub>2</sub> yields. Interestingly, the carbon yield also increased by incrementing the loadings of Cu and Zn which proved that the carbon diffusion rate of the promoted catalyst was improved as compared to the un-promoted Ni-based catalyst. This suggests that bimetallic promoters are more active catalysts as compared to monometallic promoters. Pure H<sub>2</sub> and unreacted CH<sub>4</sub> were the only gaseous products detected by gas chromatography, whereas TEM analysis confirmed the formation of MWCNT as by-product deposited on the surface of the catalyst.

Bayat et al. [90] worked on Fe–Cu promoted Ni/Al<sub>2</sub>O<sub>3</sub> catalyst. The addition of Fe and Cu in the metallic catalyst amended the catalytic stability. The promoting effect enhanced the carbon diffusion rates and hindered the formation of encapsulated carbon over the active sites. Moreover, the degree of reducibility and the dispersion of NiO on the support was also improved. The performance evaluation of the catalyst revealed that bi-promoted catalyst performed well at higher reaction temperatures. Similar results were also reported in [91] where the authors mentioned that the modification of Ni-based catalyst with Fe and Cu made it possible to carry the TCD reactions

above 973 K without affecting the physiochemical properties and stability of the materials. The effects of impregnating Ni and Co on Fe based catalyst was also studied [53] in detail, and both CH<sub>4</sub> conversions and stability of the catalyst were increased. Catalytic activity and stability of various trimetallic catalyst having different supporters and reaction conditions in FBR in TCD have been summarized in Table 3.

It can be concluded from the forementioned discussion that Ni-based catalysts are frequently used in reforming reactions due to their low cost, easy availability and highly reactive nature. The applications of these catalysts are also evident in the thermocatalytic decomposition of methane, but the only limitation that restricts industrial usage is its fast deactivation due to encapsulation of low active carbon produced as a by-product. The reaction rate of TCD is very high due to highly active nature of Ni, and hence ample amount of carbon is produced but the low diffusion rate of carbon in Ni forces the material to lose its catalytic stability and activity shortly. Hence, the impregnation of monometallic and bimetallic promoters on the Ni-based catalyst is proposed to be an active solution to this issue as explained in Sections 2.2 and 2.3 respectively.

Table 3: Catalytic activity and stability of various trimetallic catalysts having different supporters and reaction conditions in FBR in

TCD

S. No	Metal	Support	<sup>(a)</sup> W <sub>c</sub> (g)	Preparation	S.A m <sup>2</sup> g <sup>-1</sup>	<sup>(d)</sup> T <sub>R</sub> (K)	<sup>(e)</sup> R <sub>T</sub> (h)	Conversion/Yield (%)	Carbon	Ref
1.	50%Ni–5%Cu–5%Zn	MCM–22	1	IM <sup>(c)</sup>	19	1023	-	<sup>(g)</sup> 84	<sup>(i)</sup> 900	[88]
2.	50%Ni–10%Cu–10%Zn	MCM–22	1	-	19	1023	-	<sup>(g)</sup> 87	-	[89]
3.	50%Ni–15%Cu–5%Zn	MCM–22	1	-	14	1023	-	<sup>(g)</sup> 80	-	[89]
4.	50%Ni–5%Cu–15%Zn	MCM–22	1	-	12	1023	-	<sup>(g)</sup> 70	-	[89]
5.	50%Ni–15%Cu–15%Zn	MCM–22	1	-	07	1023	-	<sup>(g)</sup> 74	-	[89]
6.	30%Fe–5%Ni–10%Co	Al <sub>2</sub> O <sub>3</sub>	0.3	IM <sup>(c)</sup>	131.1	973	3	<sup>(g)</sup> 67	-	[53]
7.	30%Fe–7.5%Ni–7.5%Co	Al <sub>2</sub> O <sub>3</sub>	0.3	IM <sup>(c)</sup>	142.2	973	3	<sup>(g)</sup> 68	-	[53]
8.	30%Fe–10%Ni–5%Co	Al <sub>2</sub> O <sub>3</sub>	0.3	IM <sup>(c)</sup>	138.4	973	3	<sup>(g)</sup> 70	-	[53]
9.	50%Ni–10%Fe–5%Cu	Al <sub>2</sub> O <sub>3</sub>	0.05	IM <sup>(c)</sup>	73.3	1023	10	<sup>(g)</sup> 70	-	[90]
10.	50%Ni–10%Fe–10%Cu	Al <sub>2</sub> O <sub>3</sub>	0.05	IM <sup>(c)</sup>	59.7	1023	10	<sup>(g)</sup> 81	-	[90]
11.	50%Ni–10%Fe–15%Cu	Al <sub>2</sub> O <sub>3</sub>	0.05	IM <sup>(c)</sup>	51.0	1023	10	<sup>(g)</sup> 82	-	[90]
12.	Fe–Mo–Cu	MgO	0.5	IM <sup>(c)</sup>	67	1173	-	-	<sup>(i)</sup> 14.2	[57]

(a)Weight of catalyst (b) Fusion method (c) Impregnation method (d) Reaction temperature (e) Reaction Time (f) H<sub>2</sub> yield (g) Methane (h) g c/ g Ni (i) %

(J) mg

### 3. TCD Parameters

TCD of CH<sub>4</sub> is an endothermic process that is strongly affected by the reaction parameters, i.e. reaction temperature, GHSV, and metal loadings. It is also proposed that the morphology of the carbon deposited on the surface of the catalyst also depend upon the reaction parameters [24]. Therefore, to obtain higher CH<sub>4</sub> conversions and increase the catalyst deactivation time, it is mandatory to have an optimum set of conditions. The individual impact of independent factors of CH<sub>4</sub> decomposition has been discussed in subsequent sections.

#### 3.1. Reaction Temperature

The reaction temperature has a very significant role in the CH<sub>4</sub> conversions and catalyst stability. It is well understood that the product formation increases with the reaction temperatures due to the endothermic nature of the reaction, but the catalyst stability is affected due to the deposition of high amounts of carbon produced as a result of fast reaction rates [92].

The CH<sub>4</sub> cracking reaction by using Ni supported on SiO<sub>2</sub>, Al<sub>2</sub>O<sub>3</sub>, MgO, and ZrO<sub>2</sub> was studied by Ermakova et al. [93]. The high catalytic stability was attained at temperatures ranges of 773–823 K, but at a higher temperature (873 K), the conversions dropped rapidly. It was reported that at 873 K the rate of carbon formation as a by-product was higher than the rate of carbon diffusion. Therefore, it grew on the active sites of the catalyst resulting in their early deactivation. In another work done by Martins et al. [94], the effects of reaction temperature over Ni–Cu/SiO<sub>2</sub> were studied. The catalyst gave uniform conversions at 773 K, but the conversion declined when TCD was carried out at a temperature higher than 873 K. The possible reason for the loss in activity was found to be the sintering and encapsulation of carbon on the active sites. The effect of reaction temperature was also explored by Pinilla et al. [39]. The study was done on Fe–Mo/MgO. The results were consistent with the above discussion as the initial H<sub>2</sub> yields were increased with

reaction temperature, but with time on stream (TOS) the yields dropped. The principal reason attributed to this observation was the high reaction rate at mounted temperatures which produces ample amount of carbon. This carbon is deposited over the surface of the catalyst instead of diffusing. Moreover, at higher reaction temperatures the catalyst loses its morphology due to sintering. The H<sub>2</sub> yield at different reaction temperatures has been depicted in Fig 2.

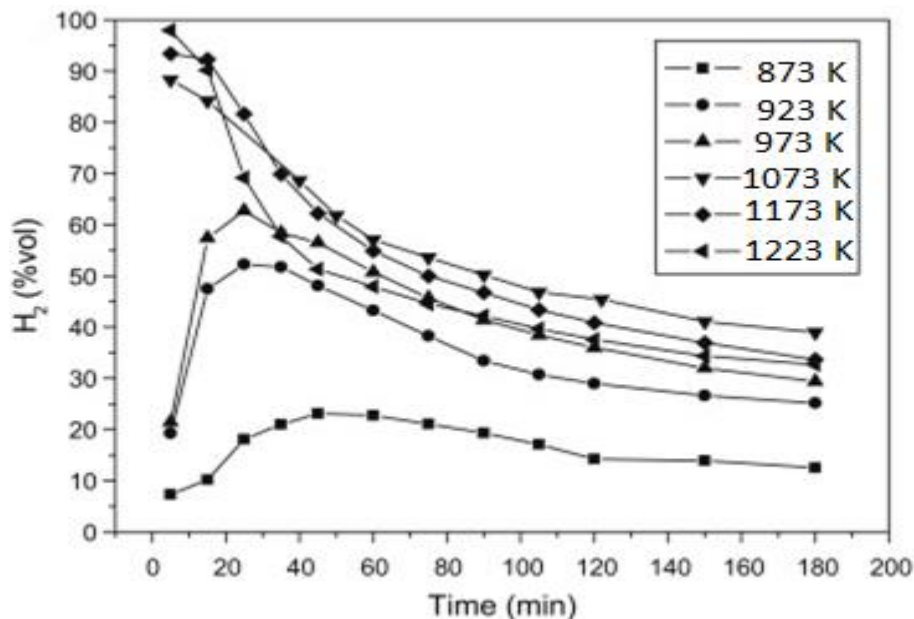


Fig 2: Influence of reaction temperature on H<sub>2</sub> yield over Fe–Mo/MgO; Reproduced with permission from Pinilla, Copyright 2011 Elsevier [39]

### 3.2. Gas Hour Space Velocity

The CH<sub>4</sub> conversions are also strongly affected by GHSV. Kumar et al. [75] studied the effect of GHSV over various catalysts. Author conducted a series of experiments to elaborate the effect of GHSV (600–3000 mL h<sup>-1</sup>g<sub>cat</sub><sup>-1</sup>) at 1023 K. The highest activity of the catalyst 50%Ni–xCu/SiO<sub>2</sub> (x= 0%, 5%, and 10%) was observed at lowest GHSV, i.e. 600 mL h<sup>-1</sup>g<sub>cat</sub><sup>-1</sup>. As the GHSV was increased, the CH<sub>4</sub> conversions and carbon yields dropped because of relatively less diffusion time available to feedstock on the active sites of the catalyst as shown in Fig 3. It was concluded that sufficient contact time of CH<sub>4</sub> with the catalyst at lower GHSV was the driving factor that resulted

in better performance. Additionally, at higher flow rates the carbon depositions are high that damage the active sites of the catalyst. To optimize the process, the flow rate should be in optimum range to provide adequate contact time to the feedstocks and to promote equilibrium between the amounts of carbon formed and diffused. Similar results were also published by Bayat et al. [73] over 50%Ni-10%Cu/Al<sub>2</sub>O<sub>3</sub> at GHSV (10,000–50,000 mL h<sup>-1</sup>g<sub>cat</sub><sup>-1</sup>) at 948 K.

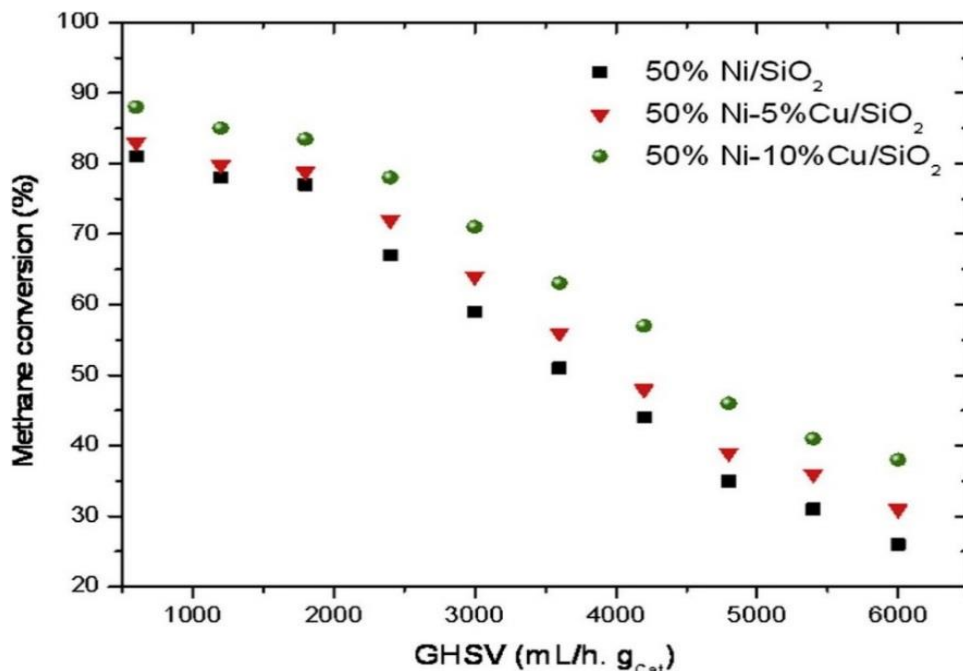


Fig 3: GHSV of reactant vs Catalytic Activity at 1023 K; Reproduced with permission from Saraswat, Copyright 2013 Elsevier [75]

### 3.3.Metal loadings

#### 3.3.1. Performance of Catalyst

The effects of metal loadings are highly significant in TCD of CH<sub>4</sub>. Manoj Pudukudy et al. [37] compared the effects of increasing metal loadings on the catalyst support. The authors impregnated 10–50% Ni on TiO<sub>2</sub> and performed TCD at 973 K. The results showed that the CH<sub>4</sub> conversions increased periodically with an increase in metal loadings. The high performance of 50%Ni/TiO<sub>2</sub> was due to the increased availability of NiO on the surface of the catalyst. The effects of increasing

the amount of Cu impregnated on Ni/Al<sub>2</sub>O<sub>3</sub> was also reported in [73]. The addition of higher amounts of Cu drastically increased the CH<sub>4</sub> conversions and catalyst stability by keeping the catalyst surface and active surface clean for CH<sub>4</sub> dissociation. By increasing the amount of Cu to 15%, an increase in CH<sub>4</sub> was observed. However, a further increase in the Cu content reduced the stability due to the quasi-liquid state of the catalyst. Similar discussions were also made by other researchers where the conversions increased linearly with the metal loading to a certain extent and then dropped drastically owing to the agglomeration of the particles [89, 90]. The CH<sub>4</sub> conversions along with metal compositions of some of the catalysts have been presented in Table 4.

Table 4: Effect of Metal Loadings \*

Sr. No	Metal Loadings	*Conversion/Yield (%)	Ref
1.	10%Ni/TiO <sub>2</sub>	<sup>(a)</sup> 27	[37]
2.	20%Ni/TiO <sub>2</sub>	<sup>(a)</sup> 30	[37]
3.	30%Ni/TiO <sub>2</sub>	<sup>(a)</sup> 33	[37]
4.	40%Ni/TiO <sub>2</sub>	<sup>(a)</sup> 37	[37]
5.	50%Ni/TiO <sub>2</sub>	<sup>(a)</sup> 42	[73]
6.	50%Ni-5%Cu/Al <sub>2</sub> O <sub>3</sub>	<sup>(b)</sup> 20	[73]
7.	50%Ni-10%Cu/Al <sub>2</sub> O <sub>3</sub>	<sup>(b)</sup> 79	[73]
8.	50%Ni-15%Cu/Al <sub>2</sub> O <sub>3</sub>	<sup>(b)</sup> 84	[73]
9.	50%Ni-10%Fe-5%Cu/Al <sub>2</sub> O <sub>3</sub>	<sup>(b)</sup> 70	[90]
10.	50%Ni-10%Fe-10%Cu/Al <sub>2</sub> O <sub>3</sub>	<sup>(b)</sup> 81	[90]

\*Dependent on reaction conditions <sup>(a)</sup> H<sub>2</sub> Yield <sup>(b)</sup> CH<sub>4</sub> Conversions

### 3.3.2. Morphology of Carbon

The effect of metal loadings on the morphology of the carbon deposited on the surface of the catalyst was discussed by Awadallah et al. [43]. The authors reported that wider CNF is formed because of impregnating higher metal loadings on the support. It is reported that the growth mechanism of CNF takes place in the following steps.

- Dissociation of CH<sub>4</sub> over the surface of the catalyst to evolve H<sub>2</sub> and elemental carbon.
- Diffusion of carbon through the metals.
- Formation of CNF on the active sites of the catalyst.

Interestingly, the metal support interaction (MSI) affected the morphology of the carbon. At low metal loadings, the base growth mechanism (BGM) dominates while in higher metal loadings, tip growth mechanism (TGM) plays its role. Therefore, larger and broader CNF and CNT are formed at higher metal loadings due to particle agglomerations and tip growth mechanism. Fig 4 shows the TEM images of carbon formed on 10%Co–Mo/Al<sub>2</sub>O<sub>3</sub> and 20%Co–Mo/Al<sub>2</sub>O<sub>3</sub> respectively.

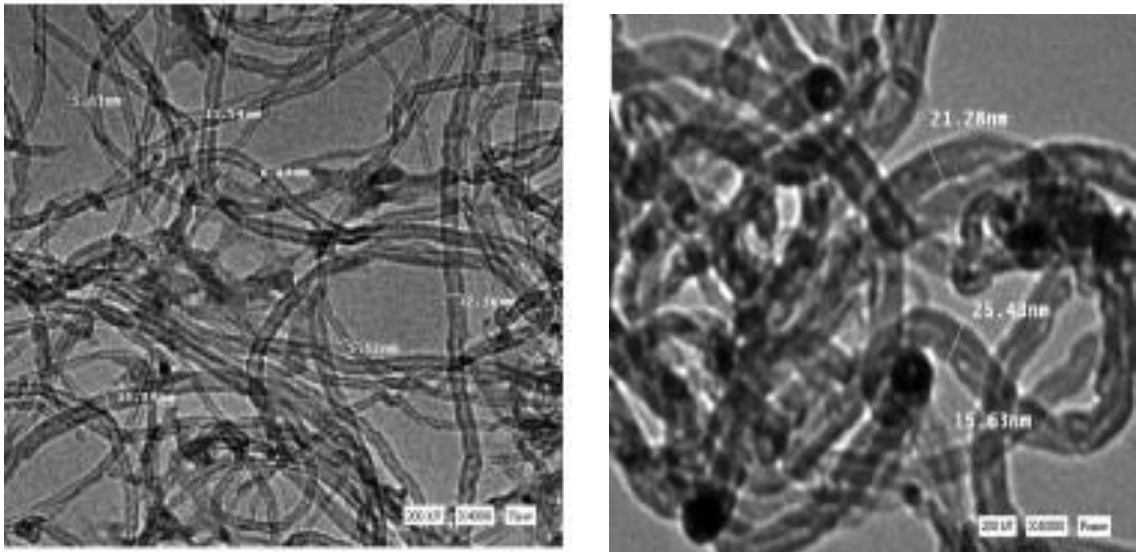


Fig.4: TEM images of carbon formed (a) 10%Co–Mo/Al<sub>2</sub>O<sub>3</sub> (b) 20%Co–Mo/Al<sub>2</sub>O<sub>3</sub>. Reproduced with permission from A. E. Awadallah, Copyright 2014 Elsevier [43]

Therefore, to obtain maximum output from the catalyst as of CH<sub>4</sub> conversions, an optimum set of reaction parameters is an essential aspect. It is believed that the increase in reaction temperatures increase the CH<sub>4</sub> conversions but, due to the high rate of reaction, an ample amount of carbon gets accumulated on the catalyst surface and deactivates it. Furthermore, the increase in GHSV restricts the catalytic activity. The low rate of CH<sub>4</sub> diffusion on the surface of the catalyst, due to the

reduced contact time between the catalyst and feedstock, is often cited as a reason behind low yield at higher space velocities. The effect of higher metal loadings and the impregnation of promoters is also worth mentioning. TCD is a catalyst-based reaction, and the overall efficiency of the reaction depends upon the active sites available for CH<sub>4</sub> adsorption. So, better results are obtained at higher metal loadings.

#### 4. TCD over admixtures as Feedstocks

TCD is an environmentally friendly technique to produce pure H<sub>2</sub> and CNF as a by-product. The major drawback of TCD limiting its industrial applications is the catalyst deactivation due to the encapsulation of less reactive carbon on the catalyst surface, which is described in the previous section [95]. The mechanism of catalyst deactivation due to deposition of carbon has been elaborated as [96, 97].

- The formation of CNF which is also called the initial stage of deactivation of the catalyst.
- The rapid deactivation of the catalyst due to the encapsulation of the active phase of the catalyst.
- The complete deactivation of the catalyst due to the detachment of metal from support.

The researchers thoroughly reviewed this problem and came up with two distinct solutions, i.e. co-feeding of CH<sub>4</sub> with other hydrocarbons and regeneration of spent catalyst by treating it with O<sub>2</sub>, CO<sub>2</sub>, and H<sub>2</sub>O at very high temperatures [98, 99]. The co-feeding of CH<sub>4</sub> with other hydrocarbons, either alternatively or collectively, enhances the catalyst deactivation [23]. These hydrocarbons produce carbon which is much more reactive as compared to carbon eliminated from CH<sub>4</sub>. The activity of carbon originating from different hydrocarbons is in of the order C<sub>benzene</sub> > C<sub>acetylene</sub> > C<sub>ethylene</sub> > C<sub>propane</sub> and C<sub>methane</sub> [100]. Limited work has been done on co-feeding of CH<sub>4</sub> with other hydrocarbons to stabilize the catalyst activity and deactivation time. Most studies are carried

out on ethane [101], C<sub>2</sub>H<sub>4</sub> [102, 103], C<sub>3</sub>H<sub>6</sub> [100], C<sub>2</sub>H<sub>5</sub>OH [104, 105], CH<sub>3</sub>OH [22, 23] and C<sub>2</sub>H<sub>2</sub> [106]. Moreover, CO<sub>2</sub> [107] and H<sub>2</sub>S [108] is also used as co-feed with CH<sub>4</sub>.

#### 4.1.Ethylene

Anna Malaika et al. [102] explored the effect of ethylene (C<sub>2</sub>H<sub>4</sub>) on the decomposition of CH<sub>4</sub> by carbon catalyzed catalysts. It was reported that although C<sub>2</sub>H<sub>4</sub> also formed a carbonaceous by-product on the surface of the catalyst as compared to CH<sub>4</sub> originated carbon; it has better catalytic properties towards CH<sub>4</sub> in CDM reactions [109]. The preliminary study without catalyst resulted in the negligible conversion of CH<sub>4</sub>. In the initial stage of the carbonaceous catalyzed reaction, the high content of H<sub>2</sub> and CH<sub>4</sub> with zero amount of C<sub>2</sub>H<sub>4</sub> showed that at initial stages of TCD, activated carbon catalyze the decomposition of C<sub>2</sub>H<sub>4</sub> as compared to CH<sub>4</sub>. With TOS, the concentrations of both CH<sub>4</sub> and C<sub>2</sub>H<sub>4</sub> reached a plateau. TCD of a mixture of CH<sub>4</sub> and C<sub>2</sub>H<sub>4</sub> is summarized in Eqs. (7)–(9).



The TCD was carried out at three different reaction temperatures, and concentration of C<sub>2</sub>H<sub>4</sub> in the feedstock and their effects on H<sub>2</sub> concentration have been explained in Fig 5. At higher reaction temperatures, the CH<sub>4</sub> conversions were relatively high as equilibrium constant moved towards products formation. For each catalyst and reaction temperature, the addition of C<sub>2</sub>H<sub>4</sub> leads to an increase in H<sub>2</sub> yield and the catalyst deactivation time was decreased. C<sub>2</sub>H<sub>4</sub> is expensive gas, and its usage in TCD reactions increases the overall operating cost of the process. Anna Malaika et al. [103] produced C<sub>2</sub>H<sub>4</sub> in situ by oxidative coupling of CH<sub>4</sub> (OCM) during TCD. The OCM reaction

was carried out over Na/CaO, or Li/MgO synthesized by the impregnation method, while the TCD catalyst was activated carbon.

The pilot study suggested that at 1123 K reaction temperature, 0.8 g of catalyst and 10% O<sub>2</sub> mixed with CH<sub>4</sub> gave higher amounts of C<sub>2</sub>H<sub>4</sub> during OCM reactions. Therefore, in the first level of TCD–OCM reaction CH<sub>4</sub> mixed with oxygen was passed over metal oxide catalyst resulting in the formation of C<sub>2</sub>H<sub>4</sub>. In the next stage, the unreacted CH<sub>4</sub> with post reaction gases was subjected to activated carbon. It was reported that although this method can be effective in restricting the deactivation of the catalyst, the formation of CO<sub>2</sub>, water vapors, and unreacted C<sub>2</sub>H<sub>6</sub> restricts its applications industrially where pure H<sub>2</sub> is required as feedstock.

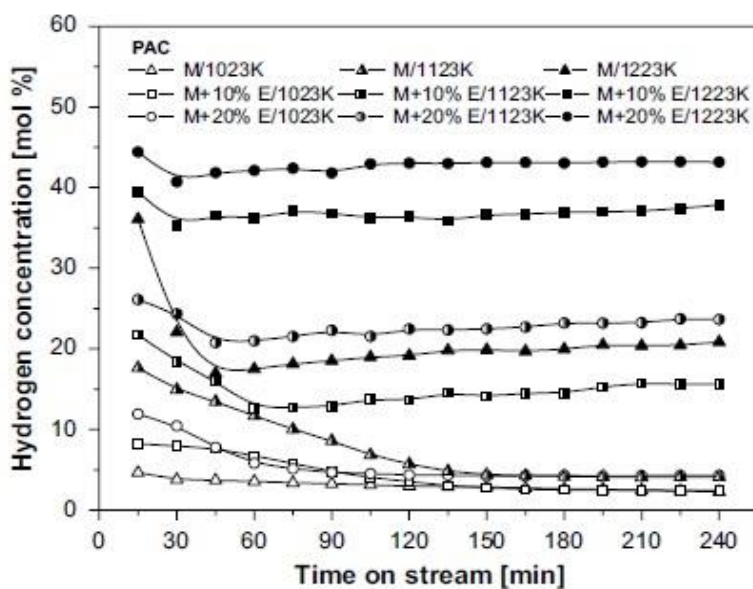


Fig 5: Influence of C<sub>2</sub>H<sub>4</sub> on H<sub>2</sub> concentrations at different reaction parameters; Reproduced with permission from A. Malaika, Copyright 2009 Elsevier [102]

#### 4.2. Propylene

The first attempt by employing propylene (C<sub>3</sub>H<sub>6</sub>) as co-feed with CH<sub>4</sub> for TCD reaction was reported by Anna Malaika et al. [100] because C<sub>3</sub>H<sub>6</sub> is cheaper than C<sub>2</sub>H<sub>4</sub> as in Fig 6. It was reported that the decomposition of C<sub>3</sub>H<sub>6</sub> results in the formation of a variety of hydrocarbons

including  $H_2$ ,  $CH_4$ ,  $C_2H_4$ ,  $C_3H_6$ ,  $C_2H_6$ , and  $C_3H_8$  thus making its reaction mechanism difficult to comprehend. Apart from the detection of these gases by chromatographic analysis of post reaction gases, the deposition of active carbon as a by-product on the surface of the catalyst was also confirmed by SEM analysis. The authors have mentioned that though  $H_2$  is produced by the catalytic decomposition of  $C_3H_6$  and  $CH_4$  while also consumed by the hydrogenation of  $C_3H_6$  and  $C_2H_4$  into  $C_3H_8$  and  $C_2H_6$  respectively. Thus, the total amount of  $H_2$  produced as the product also depends on the intake during hydrogenation reactions. The comparative study was made by using three types of activated carbon catalyst, at different reaction temperatures and different amount of  $C_3H_6$  in the feedstock. The catalyst deactivation time improved at higher reaction temperatures due to the formation of filamentous carbon on the surface of the catalyst. Fig 6 shows that the addition of  $C_3H_6$  has improved the  $H_2$  production quite significantly.

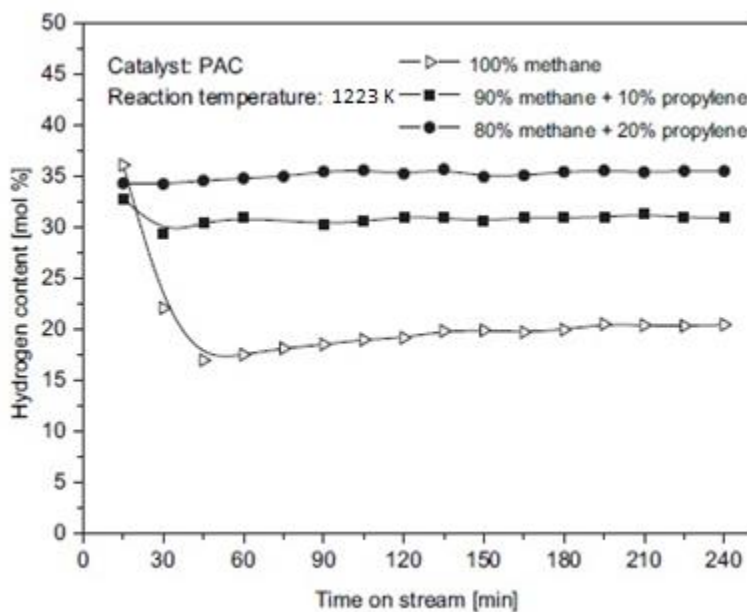


Fig 6: Influence of  $C_3H_6$  on  $H_2$  concentrations at different reaction parameters; Reproduced with permission from A. Malaika, Copyright 2010 Elsevier [100]

### **4.3. Hydrogen Sulphide**

The addition of hydrogen sulphide ( $\text{H}_2\text{S}$ ) to catalytic decomposition of  $\text{CH}_4$  is of great practical significance. The effects of adding a small number of  $\text{H}_2\text{S}$  (0.5–1 vol. %) in feedstock on  $\text{CH}_4$  decomposition over activate carbon, Ni-based catalyst and a mixture of both was investigated in [108]. It was reported that the addition of 1%  $\text{H}_2\text{S}$  increased the conversion of  $\text{CH}_4$  by 5% in the results without deactivating the carbonaceous catalyst which supports the previous study on tolerance of carbonaceous catalyst to sulphur compounds [101]. This observation makes carbon catalyst superior to the metallic catalyst in this specific area as the latter are poisoned by sulphur compounds [110]. It was also worth noted  $\text{CH}_4$  conversions were accelerated due to the formation of HS radicles which can attack  $\text{CH}_4$  molecules at higher temperatures resulting in  $\text{CH}_4$  radicles and elemental carbon.

### **4.4. Ethanol**

The effect of ethanol ( $\text{C}_2\text{H}_5\text{OH}$ ) on the catalytic decomposition of  $\text{CH}_4$  was explored by Paulina Rechnia et al. [105].  $\text{C}_2\text{H}_5\text{OH}$  was dozed alternately with  $\text{CH}_4$  at reaction temperatures of 1023–1223 K by using activated carbon as catalyst synthesized by hazelnut shells. The authors explained that apart from  $\text{H}_2$ , and unreacted  $\text{CH}_4$  in the outflow stream minor concentrations of  $\text{CO}$ ,  $\text{CO}_2$ ,  $\text{H}_2\text{O}$ , and  $\text{C}_2\text{H}_6$  were detected by gas chromatography. The preliminary study was made on the decomposition of un-diluted  $\text{CH}_4$  at different reaction temperatures. The lowest  $\text{CH}_4$  conversion was obtained at 1023 K, i.e. 3.4% that increased to 26% at 1223 K. In the next stage of the experiment,  $\text{C}_2\text{H}_5\text{OH}$  was introduced into the reactor at three different reaction temperatures. The choice of employing  $\text{C}_2\text{H}_5\text{OH}$  as an additive was based on the prior study that apart from  $\text{CH}_4$  and  $\text{H}_2$  production it also produces  $\text{C}_2\text{H}_4$  which works against catalyst deactivation [100]. The decomposition of  $\text{CH}_4$  and  $\text{C}_2\text{H}_5\text{OH}$  was carried out at the same reaction temperatures. The results

obtained at all three reaction temperatures were quite interesting. The most optimum results were obtained at 1123 K in which the cyclic addition of C<sub>2</sub>H<sub>5</sub>OH leads to an increase in CH<sub>4</sub> conversion as shown in Fig 7. It is worth noting that at 1023 K the CH<sub>4</sub> conversions decreased by the introducing C<sub>2</sub>H<sub>5</sub>OH since it was not converted completely. At 1223 K total C<sub>2</sub>H<sub>5</sub>OH and C<sub>2</sub>H<sub>4</sub> were decomposed, and a high degree of graphitization of carbon originated from CH<sub>4</sub> and C<sub>2</sub>H<sub>5</sub>OH inhibited higher CH<sub>4</sub> conversions. As the amount of C<sub>2</sub>H<sub>5</sub>OH was increased, the concentration of CO also increased. Alternatively, the production of C<sub>2</sub>H<sub>4</sub> and water as the concentration of both gases were found the same. Several other side reactions also occurred in TCD of CH<sub>4</sub> and C<sub>2</sub>H<sub>5</sub>OH. It was reported that these reactions occurred as shown in Eqs (10)–(16). [104, 111].



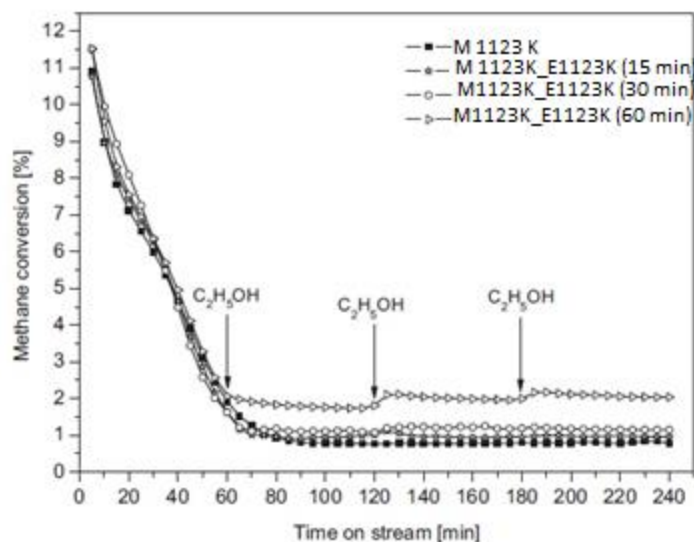


Fig 7: C<sub>2</sub>H<sub>5</sub>OH Assisted CH<sub>4</sub> decomposition at 1123 K; Reproduced with permission from P.

Rechnia, Copyright 2012 Elsevier [105]

#### 4.5.2% Methanol/Methane

The effect of 2% premixed methanol in methane used as feedstock for TCD has been explored by our group. Different composition of Ni-based catalyst was synthesized by wet impregnation method [142]. The results showed that methane conversions increased proportionally with metal loadings and 50%Ni/Al<sub>2</sub>O<sub>3</sub> gave the best results. Additionally, the addition of Pd on Ni-based catalyst having drastic effects on the activity and stability of the catalyst was also reported [149]. Furth more, the activity and stability of Cu promoted Ni-based catalyst was also evaluated in [112]

### 5. Kinetics and reaction mechanism of TCD

Kinetic studies are often done to find an appropriate reaction rate model that correlates the experimental data, describes the rate of reaction, the order of reaction and activation energies [113]. The proper understanding of kinetics models can further optimize the catalyst design and improves the overall efficiency of the process concerning CH<sub>4</sub> consumption rates and carbon depositions. SRM is often termed as one of the early methods used in industries for H<sub>2</sub> production,

but the formation of ample amount of greenhouse gases opens the floor for further research in finding an environment for H<sub>2</sub> production [114]. TCD of CH<sub>4</sub> is widely explored by scholars, and a series of catalysts are being synthesized reported in the literature (c.f. Table 1-3) having specific reaction order and activation energies (c.f. Table 5) [115]. Ashik et al. [116] thoroughly studied the reaction mechanism of TCD over Ni/SiO<sub>2</sub> nanocatalyst prepared by co-precipitation cum modified Stober method. The studies were made around the reaction temperature of 823–923 K and pressure of 21–81 kPa. The CH<sub>4</sub> conversions increased with reaction temperature and partial pressures, but the catalyst was subjected to an early deactivation due to the formation of CNF resulted in high reaction rates at higher temperatures as shown in Fig 8.

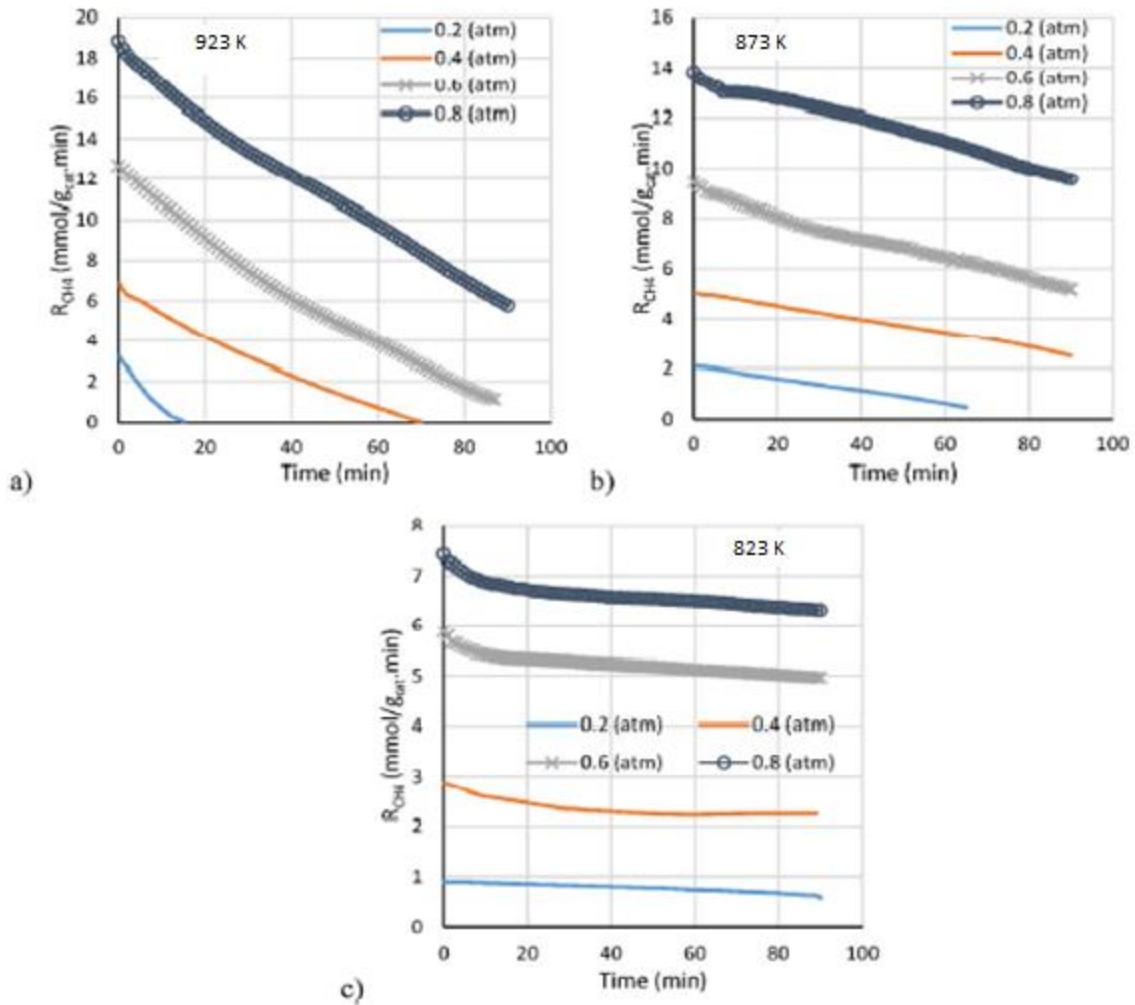


Fig 8: Reaction time vs CH<sub>4</sub> decomposition; Reproduced with permission from U. Ashik, Copyright 2017 Elsevier [116]

The authors reported that as the TCD of CH<sub>4</sub> occurs in various steps and the reaction kinetics of each step is still under study, this makes the overall mechanism of TCD extremely complicated. Empirical model law based on power law was used in this study for computing the reaction order and activation energy. In another study, the reaction kinetics over Ni–Cu–Co was studied, and the activation energy was calculated by Arrhenius plot shown in Fig 9 [117].

Recent studied made by [118] reported that the initial step of CH<sub>4</sub>, i.e. breakage of bonds in TCD over the metallic catalyst is the rate determining step since the activation energy decreased from

440 kJ mol<sup>-1</sup> to 65 kJ mol<sup>-1</sup> over Ni (100) catalyst at high temperatures. Similarly, Maryam et al. [119] carried kinetic modelling of CH<sub>4</sub> decomposition at a temperature range of 823–923 K over Ni–Cu/MgO and estimated around 50.4 kJ mol<sup>-1</sup> of activation energy. The results also revealed that the catalyst deactivation was dependent on TOS, reaction temperature, and partial pressures. Nasir et al. [96] stated that a reaction order and activation energy of 2.65 and 61.77 kJ mol<sup>-1</sup> respectively was obtained by carrying out TCD over Ni/Zeolite catalyst. The kinetic data indicated that the optimum reaction temperature and partial CH<sub>4</sub> pressures must be maintained to get the highest performance from the catalyst in terms of catalyst activity and stability.

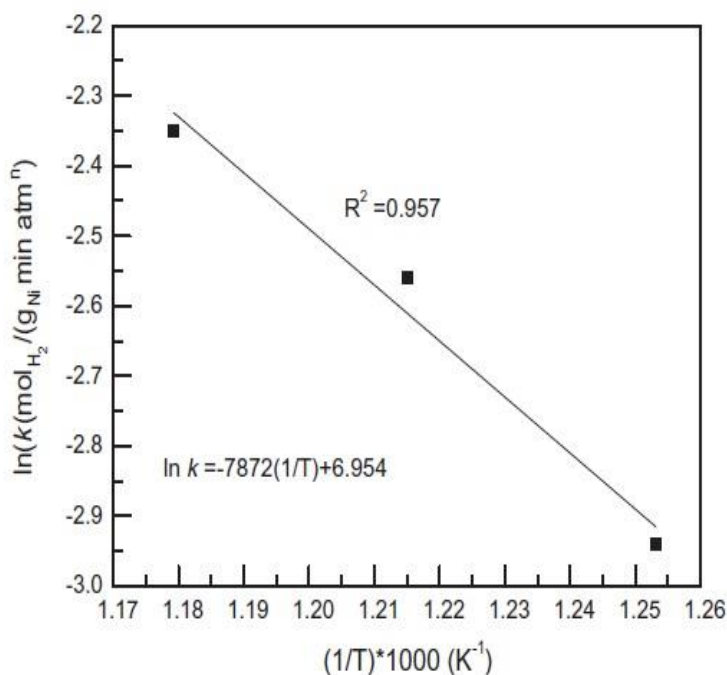


Fig 9: Activation Plot of Ni–Cu–Co; Reproduced with permission from H. Y. Wang, Copyright 2014

Elsevier [117]

The activation energy and order of reaction of some of the highly active catalyst in TCD of CH<sub>4</sub> has been shown in Table 5.

Table 5: Activation Energy of First-order TCD over Metal Based Catalyst by Empirical Model

Catalyst	Activation Energy E <sub>a</sub> (kJ mole <sup>-1</sup> ) <sup>(a)</sup>	Ref
Ni	65.4	[117]
Ni	64.6	[120]
Ni/Zeolite	61.77	[96]
Ni/TiO <sub>2</sub>	60	[121]
Ni/SiO <sub>2</sub>	29.5	[122]
Ni–Cu/Al <sub>2</sub> O <sub>3</sub>	46	[123]
Ni–Cu/MgO	50.4	[119]
Ni–Cu–Co	67.5	[117]

<sup>(a)</sup>Dependent Upon Reaction Parameters

The comparison of different hydrogen production techniques has been furnished in Table 6. The liberation of ample amount of greenhouse gases marks SRM, DRM and POM unfavorable techniques for H<sub>2</sub> production. Moreover, the separation of H<sub>2</sub> from synthesis gas requires heavy equipment that increases the overall cost of the process. TCD is a nonoxidative technique in which CH<sub>4</sub> is decomposed into H<sub>2</sub> and elemental carbon as a by-product. Furthermore, among all suggested processes TCD occurs at the lowest reaction temperature because metallic catalysts are used.

Table 6: Comparison in between H<sub>2</sub> Production Techniques

	SRM	DRM	POM	TCD
Reaction	$\text{CH}_4 + \text{H}_2\text{O} \rightarrow \text{CO} + 3\text{H}_2$	$\text{CH}_4 + \text{CO}_2 \rightarrow 2\text{CO} + 2\text{H}_2$	$\text{CH}_4 + 0.5 \text{O}_2 \rightarrow \text{CO} + 2\text{H}_2$	$\text{CH}_4 \rightarrow \text{C} + 2\text{H}_2$
Advantages	<ol style="list-style-type: none"> <li>1.75-85% Efficiency</li> <li>2.Ancient Technique</li> </ol>	<ol style="list-style-type: none"> <li>1. Two green House gases are consumed, i.e. CH<sub>4</sub> and CO<sub>2</sub></li> <li>2. Clean fuel is a product</li> </ol>	<ol style="list-style-type: none"> <li>1.60-75% Efficiency</li> <li>2. Low Residence Time</li> <li>3.High Reaction Yield</li> </ol>	<ol style="list-style-type: none"> <li>1. Green and Nonoxidative Technique.</li> <li>2.Highly ordered carbon produced as a by-product.</li> </ol>
Disadvantages	<ol style="list-style-type: none"> <li>1.Costly process.</li> <li>2.High reaction temperature and pressure required</li> <li>3. H<sub>2</sub> must be removed from synthesis gas</li> </ol>	<ol style="list-style-type: none"> <li>1. Carbon formation and sintering.</li> <li>2. H<sub>2</sub> must be removed from synthesis gas.</li> </ol>	<ol style="list-style-type: none"> <li>1. Costly technique as it requires the cryogenic unit to sperate O<sub>2</sub> from Air</li> <li>2. H<sub>2</sub> must be removed from synthesis gas</li> </ol>	<ol style="list-style-type: none"> <li>1. Deactivation of the catalyst due to encapsulation of low active carbon.</li> </ol>
H <sub>2</sub> /CO Ratio	H <sub>2</sub> /CO Ratio: 3:1	H <sub>2</sub> /CO Ratio: 1:1	H <sub>2</sub> /CO Ratio: 2:1	H <sub>2</sub> /CO Ratio: -
Operating Temperature	973-1273 K	1223-1373 K	923-1023 K	823-1023 K
Operating Pressure	3-25 bar	1 bar	100 bar	1 bar

## 6. Outlook

TCD has been termed as one of the effective technique to produce CO<sub>x</sub> free H<sub>2</sub> that can replace all existing fuels due to clean and abundant energy. The hydrogen produced by this process can be directly employed as feedstock in fuel cells while carbon obtained as by-product can be used as advanced materials and catalysts. The main problems encountered in this process as stated in literature surveys are high reaction temperature, and rapid catalyst deactivation as the formation of carbon destabilizes the adsorption capacity of clean material thus lowering its catalytic activity and stability. In recent years, cumulative efforts have been devoted for the commercialization of TCD, and reaction kinetics, catalyst developments and process parameters have been investigated broadly. However, this process needs further directions. The current article enlightens that TCD can be developed by further theoretical and experimental investigations. It is considered that the future perspective of TCD research is to concentrate on the synthesis of trimetallic catalysts having suitable metals comprising of appropriate compositions. The impregnation of Mo, Co, Fe, Cu, Pd, Cr and Pt on the Ni-based catalyst can serve the purpose of industrializing TCD. Furthermore, the mixtures of CH<sub>4</sub> with other hydrocarbons like C<sub>6</sub>H<sub>6</sub>, H<sub>2</sub>S, CO<sub>2</sub>, alkanes, and alkanols can be utilized as efficient feedstocks for TCD as it gives better hydrogen yields and improve carbon types towards MWCNTs. The synthesis methods, calcination temperatures, and activation temperatures are also essential to enhance the performance of the catalysts. The suitable synthesis techniques and activation conditions can give a high dispersion of metal on support, robust metal support activation and high resistance to coke. Additionally, the reactor designs must be explored deeply to optimize this process. It is believed that a practical research done on these parameters can give better results in the respective fields. This will help to get ample energy by the combustion

of H<sub>2</sub> by industrializing TCD of CH<sub>4</sub>. It is also worth mentioning that, industrialization of TCD will assist to tackle the issue of clean energy crisis and GHG emissions which is the root cause of global warming. Moreover, the carbon produced as a by-product will serve as a value-added product as catalyst and power generation.

## **7. Conclusion**

TCD has been considered as green and economical method to produce pure H<sub>2</sub> and elemental carbon as a by-product without the need of a costly separation method as compared to other techniques, i.e. DRM, SRM and POM. However, a high reaction temperature of TCD and fast deactivation of the catalyst has restricted this process for commercial applications. For this purpose, the metal-based catalysts, i.e. noble and transition metals have been extensively researched to lower the reaction temperature and improve the catalyst stability. Ni, Cu, Co, Fe, and Pd are the most studied transition metals impregnated on Al<sub>2</sub>O<sub>3</sub>, FeO, MgO, CeO<sub>2</sub>, and La<sub>2</sub>O<sub>3</sub>. Of all metallic catalysts, Ni-based materials proved to be better due to its low cost, easy availability and excellent catalytic efficiency as compared to other metals. While parameters such as reaction temperature, GHSV, and metal loading also affect the process yields. The co-feeding of CH<sub>4</sub> with other feedstock C<sub>2</sub>H<sub>4</sub>, C<sub>3</sub>H<sub>6</sub>, C<sub>2</sub>H<sub>5</sub>OH and CH<sub>3</sub>OH producing more active carbon as a by-product is proposed to be effective solution to overcome the rapid catalyst deactivation. Lastly, the kinetic study is presented in which the research done by some notable's groups were mentioned based on activation energies. An empirical model based on the power law is considered as the most appropriate model that fits in TCD, and hence the order of reaction and activation energy is calculated.

## Acknowledgement

The authors gratefully acknowledge Universiti Teknologi PETRONAS, Malaysia in providing the necessary facilities to conduct the work.

## References

- [1] H. Y. Wang and A. C. Lua, "Development of metallic nickel nanoparticle catalyst for the decomposition of methane into hydrogen and carbon nanofibers," *The Journal of Physical Chemistry C*, 2012.116, 26765-26775.
- [2] G. Nicoletti, N. Arcuri, G. Nicoletti, and R. Bruno, "A technical and environmental comparison between hydrogen and some fossil fuels," *Energy Conversion and Management*, 2015. 89, 205-213.
- [3] G. Supran and N. Oreskes, "Assessing ExxonMobil's climate change communications (1977–2014)," 2017, 12.
- [4] S. N. Khan, S. M. Hailegiorgis, Z. Man, A. M. Shariff, and S. Garg, "Thermophysical properties of concentrated aqueous solution of N-methyldiethanolamine (MDEA), piperazine (PZ), and ionic liquids hybrid solvent for CO<sub>2</sub> capture," *Journal of Molecular Liquids*, 2017. 229, 221-229.
- [5] M. Shaikh, A. Shariff, M. Bustam, and G. Murshid, "Measurement and prediction of physical properties of aqueous sodium l-prolinate and piperazine as a solvent blend for CO<sub>2</sub> removal," *Chemical Engineering Research and Design*, 2015, 102, 378-38.
- [6] S. N. Khan, S. M. Hailegiorgis, Z. Man, A. M. Shariff, and S. Garg, "Thermophysical properties of aqueous N-methyldiethanolamine (MDEA) and ionic liquids 1-butyl-3-methylimidazolium trifluoromethanesulfonate [bmim][OTf], 1-butyl-3-

- methylimidazolium acetate [bmim][Ac] hybrid solvents for CO<sub>2</sub> capture," *Chemical Engineering Research and Design*, 2017. 121, 69-80.
- [7] F. Iqbal, M. I. A. Mutalib, M. S. Shaharun, and B. Abdullah, "Synthesis of ZnFe<sub>2</sub>O<sub>4</sub> Using sol-gel Method: Effect of Different Calcination Parameters," *Procedia Engineering*, 2016. 148, . 787-794.
- [8] I. Jain, "Hydrogen the fuel for 21st century," *International journal of hydrogen energy*, 2009, 34, 7368-737.
- [9] H. F. Abbas and W. W. Daud, "Hydrogen production by methane decomposition: a review," *International Journal of Hydrogen Energy*, 2010,35, 160-1190.
- [10] M. Ball and M. Wietschel, "The future of hydrogen—opportunities and challenges," *International journal of hydrogen energy*, 2009. 34, 615-62.
- [11] M. Balat and M. Balat, "Political, economic and environmental impacts of biomass-based hydrogen," *International journal of hydrogen energy*, 2009, 34, 3589-3603.
- [12] H. Ong, T. Mahlia, and H. Masjuki, "A review on energy scenario and sustainable energy in Malaysia," *Renewable and Sustainable Energy Reviews*, 2011 15, 639-647.
- [13] B. Abdullah, N. A. A. Ghani, and D.-V. N. Vo, "Recent Advances in Dry Reforming of Methane over Ni-based Catalysts," *Journal of Cleaner Production*, 2017 162. 170-185.
- [14] I. S. Locka, S. S. Lockb, N. Dai-viet, and B. Abdullah, "Influence of Palladium on Ni-based Catalyst for Hydrogen Production via Thermo-catalytic Methane Decomposition," *CHEMICAL ENGINEERING*, 2017, 57.
- [15] U. Sikander, S. Sufian, and M. Salam, "A review of hydrotalcite based catalysts for hydrogen production systems," *International Journal of Hydrogen Energy*, 2017. 42, 19851-19868.

- [16] Z. Khan, S. Yusup, M. M. Ahmad, V. S. Chok, Y. Uemura, and K. M. Sabil, "Review on hydrogen production technologies in Malaysia," *International Journal of Engineering & Technology*, 2010, 10.
- [17] Y. Li, D. Li, and G. Wang, "Methane decomposition to CO x-free hydrogen and nano-carbon material on group 8–10 base metal catalysts: a review," *Catalysis today*, 2011, 162, 1-48.
- [18] M. Ermakova, D. Y. Ermakov, and G. Kuvshinov, "Effective catalysts for direct cracking of methane to produce hydrogen and filamentous carbon: Part I. Nickel catalysts," *Applied Catalysis A: General*, 2000, 201, 61-70.
- [19] H. J. Alves, C. B. Junior, R. R. Niklevicz, E. P. Frigo, M. S. Frigo, and C. H. Coimbra-Araújo, "Overview of hydrogen production technologies from biogas and the applications in fuel cells," *international journal of hydrogen energy*, 2013. 38, 5215-5225.
- [20] U. Ashik, W. W. Daud, and H. F. Abbas, "Production of greenhouse gas free hydrogen by thermocatalytic decomposition of methane—A review," *Renewable and Sustainable Energy Reviews*, 2015, 44, 221-256,.
- [21] K. Srilatha, D. Bhagawan, S. S. Kumar, and V. Himabindu, "Sustainable fuel production by thermocatalytic decomposition of methane—A review," *South African Journal of Chemical Engineering*, 2017. 24, 156-167.
- [22] A. Awad, A. Salam, and B. Abdullah, "Hydrogen Production by Decomposition of Methane and Methanol Mixture over Ni-Pd/Al<sub>2</sub>O<sub>3</sub>," *Journal of the Japan Institute of Energy*, 2017, 445-450.

- [23] A. Awad, A. Salam, and B. Abdullah, "Thermocatalytic decomposition of methane/methanol mixture for hydrogen production: Effect of nickel loadings on alumina support," in *AIP Conference Proceedings*, 2017, p. 020030.
- [24] I. Suelves, M. Lázaro, R. Moliner, B. Corbella, and J. Palacios, "Hydrogen production by thermo catalytic decomposition of methane on Ni-based catalysts: influence of operating conditions on catalyst deactivation and carbon characteristics," *International Journal of Hydrogen Energy*, 2015. 30, 1555-1567.
- [25] M. A. Salam and B. Abdullah, "Catalysis mechanism of Pd-promoted  $\gamma$ -alumina in the thermal decomposition of methane to hydrogen: A density functional theory study," *Materials Chemistry and Physics*, 2017, 188, 18-23.
- [26] U. Ashik, W. W. Daud, and J.-i. Hayashi, "A review on methane transformation to hydrogen and nanocarbon: Relevance of catalyst characteristics and experimental parameters on yield," *Renewable and Sustainable Energy Reviews*, 2017, 76, 743-767.
- [27] L. Zhou, L. R. Enakonda, M. Harb, Y. Saih, A. Aguilar-Tapia, S. Ould-Chikh, *et al.*, "Fe catalysts for methane decomposition to produce hydrogen and carbon nano materials," *Applied Catalysis B: Environmental*, 2015, 208, 44-59.
- [28] A. A. Ibrahim, A. H. Fakeeha, A. S. Al-Fatesh, A. E. Abasaheed, and W. U. Khan, "Methane decomposition over iron catalyst for hydrogen production," *International Journal of Hydrogen Energy*, 2015. 40, 7593-7600.
- [29] A. H. Fakeehaa, A. A. Ibrahima, A. S. Al Fatesha, W. U. Khana, Y. A. Mohammeda, A. E. Abasaeeda, *et al.*, "Fe Supported Alumina Catalyst for Methane Decomposition: Effect of Co Coupling," *Int. J. of Sustainable Water & Environmental Systems*, 2016. 8,00-00.

- [30] S. Takenaka, H. Ogihara, I. Yamanaka, and K. Otsuka, "Decomposition of methane over supported-Ni catalysts: effects of the supports on the catalytic lifetime," *Applied Catalysis A: General*, 2001, 217, 101-110.
- [31] N. Bayat, M. Rezaei, and F. Meshkani, "CO<sub>x</sub>-free hydrogen and carbon nanofibers production by methane decomposition over nickel-alumina catalysts," *Korean Journal of Chemical Engineering*, 2016, 33, 490-49.
- [32] S. Makvandi and S. Alavi, "CO<sub>x</sub> free hydrogen production by catalytic decomposition of methane over porous Ni/Al<sub>2</sub>O<sub>3</sub> catalysts," *Iranian Journal of Chemical Engineering*, 2011. 8, 24-33.
- [33] W. Ahmed, M. N. El-Din, A. Aboul-Enein, and A. Awadallah, "Effect of textural properties of alumina support on the catalytic performance of Ni/Al<sub>2</sub>O<sub>3</sub> catalysts for hydrogen production via methane decomposition," *Journal of Natural Gas Science and Engineering*, 2015. 25, 359-366.
- [34] J. F. Pola, M. A. Valenzuela, I. A. Córdova, and J. Wang, "Hydrogen production via methane decomposition using Ni and Ni-Cu catalysts supported on MgO, Al<sub>2</sub>O<sub>3</sub> and MgAl<sub>2</sub>O<sub>4</sub>," *MRS Online Proceedings Library Archive*, 2010, 1279.
- [35] M. Pudukudy, Z. Yaakob, and M. S. Takriff, "Methane decomposition into CO<sub>x</sub> free hydrogen and multiwalled carbon nanotubes over ceria, zirconia and lanthana supported nickel catalysts prepared via a facile solid state citrate fusion method," *Energy Conversion and Management*, 2016 126, 302-315.
- [36] S. Takenaka, H. Ogihara, and K. Otsuka, "Structural change of Ni species in Ni/SiO<sub>2</sub> catalyst during decomposition of methane," *Journal of Catalysis*, 202. 208, 54-63.

- [37] M. Pudukudy, Z. Yaakob, A. Kadier, M. S. Takriff, and N. S. M. Hassan, "One-pot sol-gel synthesis of Ni/TiO<sub>2</sub> catalysts for methane decomposition into CO<sub>x</sub> free hydrogen and multiwalled carbon nanotubes," *International Journal of Hydrogen Energy*, 2017, 42, 16495-16513.
- [38] A. E. Awadallah, M. S. Mostafa, A. A. Aboul-Enein, and S. A. Hanafi, "Hydrogen production via methane decomposition over Al<sub>2</sub>O<sub>3</sub>-TiO<sub>2</sub> binary oxides supported Ni catalysts: Effect of Ti content on the catalytic efficiency," *Fuel*, 2014, 129, 68-77.
- [39] J. Pinilla, R. Utrilla, R. Karn, I. Suelves, M. Lázaro, R. Moliner, *et al.*, "High temperature iron-based catalysts for hydrogen and nanostructured carbon production by methane decomposition," *International Journal of hydrogen energy*, 2011, 36, 7832-7843.
- [40] A. A. Ibrahim, A. S. Al-Fatesh, W. U. Khan, M. A. Soliman, A. Otaibi, L. Raja, *et al.*, "Influence of support type and metal loading in methane decomposition over iron catalyst for hydrogen production," *Journal of the Chinese Chemical Society*, 2015, 62, 592-599.
- [41] A. H. Fakeeha, A. A. Ibrahim, W. U. Khan, K. Seshan, R. L. Al Otaibi, and A. S. Al-Fatesh, "Hydrogen production via catalytic methane decomposition over alumina supported iron catalyst," *Arabian Journal of Chemistry*, 2016, 11, 405-41.
- [42] A. E. Awadallah and A. A. Aboul-Enein, "Catalytic decomposition of methane to CO<sub>x</sub>-free hydrogen and carbon nanotubes over Co-W/MgO catalysts," *Egyptian Journal of Petroleum*, 2015, 24, 299-30.
- [43] A. E. Awadallah, A. A. Aboul-Enein, and A. K. Aboul-Gheit, "Effect of progressive Co loading on commercial Co-Mo/Al<sub>2</sub>O<sub>3</sub> catalyst for natural gas decomposition to CO<sub>x</sub>-free hydrogen production and carbon nanotubes," *Energy Conversion and Management*, 2014, 77, 143-15.

- [44] L. Tang, D. Yamaguchi, N. Burke, D. Trimm, and K. Chiang, "Methane decomposition over ceria modified iron catalysts," *Catalysis Communications*, 2010,11, 1215-1219.
- [45] A. E. Awadallah, A. A. Aboul-Enein, and A. K. Aboul-Gheit, "Impact of group VI metals addition to Co/MgO catalyst for non-oxidative decomposition of methane into CO<sub>x</sub>-free hydrogen and carbon nanotubes," *Fuel*, vol. 129, 27-36.
- [46] A. E. Awadallah, M. S. Abdel-Mottaleb, A. A. Aboul-Enein, M. M. Yonis, and A. K. Aboul-Gheit, "Catalytic decomposition of natural gas to CO/CO<sub>2</sub>-free hydrogen production and carbon nanomaterials using mgO-Supported monometallic iron family catalysts," *Chemical Engineering Communications*,2015, 202, 163-174.
- [47] M. Pudukudy and Z. Yaakob, "Methane decomposition over Ni, Co and Fe based monometallic catalysts supported on sol gel derived SiO<sub>2</sub> microflakes," *Chemical Engineering Journal*, 2015, 262,1009-1021.
- [48] A. Awadallah, A. Aboul-Enein, D. El-Desouki, and A. Aboul-Gheit, "Catalytic thermal decomposition of methane to CO<sub>x</sub>-free hydrogen and carbon nanotubes over MgO supported bimetallic group VIII catalysts," *Applied Surface Science*, 2014, 296, 100-10.
- [49] M. Pudukudy, Z. Yaakob, and Z. S. Akmal, "Direct decomposition of methane over Pd promoted Ni/SBA-15 catalysts," *Applied Surface Science*, 2015, 353, 127-136.
- [50] M. Pudukudy, Z. Yaakob, and M. S. Takriff, "Methane decomposition over Pd promoted Ni/MgAl<sub>2</sub>O<sub>4</sub> catalysts for the production of CO<sub>x</sub> free hydrogen and multiwalled carbon nanotubes," *Applied Surface Science*, 2015, 356, 1320-1326.
- [51] A. Awadallah, A. Aboul-Enein, M. Yonis, and A. Aboul-Gheit, "Effect of structural promoters on the catalytic performance of cobalt-based catalysts during natural gas

- decomposition to hydrogen and carbon nanotubes," *Fullerenes, Nanotubes and Carbon Nanostructures*, 2016, 24, 181-18.
- [52] R. R. Silva, H. A. Oliveira, A. C. Guarino, B. B. Toledo, M. B. Moura, B. T. Oliveira, *et al.*, "Effect of support on methane decomposition for hydrogen production over cobalt catalysts," *International Journal of Hydrogen Energy*, 2016, 41,6763-6772.
- [53] A. Al-Fatesh, A. Fakeeha, W. Khan, A. Ibrahim, S. He, and K. Seshan, "Production of hydrogen by catalytic methane decomposition over alumina supported mono-, bi-and tri-metallic catalysts," *International Journal of Hydrogen Energy*, 2016. 41, 22932-22940.
- [54] M. Pudukudy, A. Kadier, Z. Yaakob, and M. S. Takriff, "Non-oxidative thermocatalytic decomposition of methane into CO<sub>x</sub> free hydrogen and nanocarbon over unsupported porous NiO and Fe<sub>2</sub>O<sub>3</sub> catalysts," *International Journal of Hydrogen Energy*, 2016, 41,18509-18521.
- [55] I. L. S. Mei, S. Lock, D.-V. N. Vo, and A. Bawadi, "Thermo-Catalytic Methane Decomposition for Hydrogen Production: Effect of Palladium Promoter on Ni-based Catalysts," *Bulletin of Chemical Reaction Engineering & Catalysis*,2016. 11, 191-199.
- [56] M. Pudukudy, Z. Yaakob, M. Z. Mazuki, M. S. Takriff, and S. S. Jahaya, "One-pot sol-gel synthesis of MgO nanoparticles supported nickel and iron catalysts for undiluted methane decomposition into CO<sub>x</sub> free hydrogen and nanocarbon," *Applied Catalysis B: Environmental*, 2017, 218298-316.
- [57] A. E. Awadallah, A. A. Aboul-Enein, M. A. Azab, and Y. K. Abdel-Monem, "Influence of Mo or Cu doping in Fe/MgO catalyst for synthesis of single-walled carbon nanotubes by catalytic chemical vapor deposition of methane," *Fullerenes, Nanotubes and Carbon Nanostructures*, 2017, 25, 256-264.

- [58] C. Anjaneyulu, S. N. Kumar, V. V. Kumar, G. Naresh, S. Bhargava, K. Chary, *et al.*, "Influence of La on reduction behaviour and Ni metal surface area of Ni–Al<sub>2</sub>O<sub>3</sub> catalysts for CO<sub>x</sub> free H<sub>2</sub> by catalytic decomposition of methane," *international journal of hydrogen energy*, 2015, 40,3633-364.
- [59] A. Venugopal, S. N. Kumar, J. Ashok, D. H. Prasad, V. D. Kumari, K. Prasad, *et al.*, "Hydrogen production by catalytic decomposition of methane over Ni/SiO<sub>2</sub>," *International Journal of Hydrogen Energy*, 2007 32, 1782-1788.
- [60] Y. Echegoyen, I. Suelves, M. Lazaro, R. Moliner, and J. Palacios, "Hydrogen production by thermocatalytic decomposition of methane over Ni-Al and Ni-Cu-Al catalysts: Effect of calcination temperature," *Journal of Power Sources*, 2007, 169, 150-157.
- [61] Y. Echegoyen, I. Suelves, M. Lázaro, M. Sanjuán, and R. Moliner, "Thermo catalytic decomposition of methane over Ni–Mg and Ni–Cu–Mg catalysts: effect of catalyst preparation method," *Applied Catalysis A: General*, 2007, 333, 229-237.
- [62] M. J. Lázaro, Y. Echegoyen, I. Suelves, J. M. Palacios, and R. Moliner, "Decomposition of methane over Ni-SiO<sub>2</sub> and Ni-Cu-SiO<sub>2</sub> catalysts: effect of catalyst preparation method," *Applied Catalysis A: General*, 2007, 329, 22-29.
- [63] M. Lazaro, Y. Echegoyen, C. Alegre, I. Suelves, R. Moliner, and J. Palacios, "TiO<sub>2</sub> as textural promoter on high loaded Ni catalysts for methane decomposition," *International Journal of hydrogen energy*, 2008, 33, 3320-3329.
- [64] A. E. Awadallah, F. K. Gad, A. A. Aboul-Enein, M. R. Labib, and A. K. Aboul-Gheit, "Direct conversion of natural gas into CO<sub>x</sub>-free hydrogen and MWCNTs over commercial Ni–Mo/Al<sub>2</sub>O<sub>3</sub> catalyst: Effect of reaction parameters," *Egyptian Journal of Petroleum*, 2013. 22, 27-34,.

- [65] A. E. Awadallah, A. A. Aboul-Enein, and A. K. Aboul-Gheit, "Various nickel doping in commercial Ni–Mo/Al<sub>2</sub>O<sub>3</sub> as catalysts for natural gas decomposition to CO<sub>x</sub>-free hydrogen production," *Renewable energy*, 2013,57, 671-678.
- [66] W. Ahmed, A. E. Awadallah, and A. A. Aboul-Enein, "Ni/CeO<sub>2</sub>–Al<sub>2</sub>O<sub>3</sub> catalysts for methane thermo-catalytic decomposition to CO<sub>x</sub>-free H<sub>2</sub> production," *International Journal of Hydrogen Energy*, 2016, 41, 18484-18493.
- [67] A.-S. Al-Fatesh, S. Barama, A.-A. Ibrahim, A. Barama, W.-U. Khan, and A. Fakeeha, "Study of Methane Decomposition on Fe/MgO-Based Catalyst Modified by Ni, Co, and Mn Additives," *Chemical Engineering Communications*, 2017.1-11
- [68] A. S. Al-Fatesh, A. Amin, A. A. Ibrahim, W. U. Khan, M. A. Soliman, R. L. AL-Otaibi, *et al.*, "Effect of Ce and Co addition to Fe/Al<sub>2</sub>O<sub>3</sub> for catalytic methane decomposition," *Catalysts*, 2016. 6, 40
- [69] A. H. Fakeeha, W. U. Khan, A. S. Al-Fatesh, A. E. Abasaheed, and M. A. Naeem, "Production of hydrogen and carbon nanofibers from methane over Nie CoeAl catalysts," *Int J Hydrogen Energy*, 2015, 40,81.
- [70] A. Al-Fatesh, A. Fakeeha, A. Ibrahim, W. Khan, H. Atia, R. Eckelt, *et al.*, "Decomposition of methane over alumina supported Fe and Ni–Fe bimetallic catalyst: Effect of preparation procedure and calcination temperature," *Journal of Saudi Chemical Society*, 2016, 22, 239-247.
- [71] W. U. Khan, A. H. Fakeeha, A. S. Al-Fatesh, A. A. Ibrahim, and A. E. Abasaheed, "La<sub>2</sub>O<sub>3</sub> supported bimetallic catalysts for the production of hydrogen and carbon nanomaterials from methane," *International Journal of Hydrogen Energy*, 2015, 41, 976-983

- [72] A. H. Fakeeha, W. U. Khan, A. S. Al-Fatesh, A. A. Ibrahim, and A. E. Abasaheed, "Production of hydrogen from methane over lanthanum supported bimetallic catalysts," *International Journal of Hydrogen Energy*, 2016, 41, 8193-8198.
- [73] N. Bayat, M. Rezaei, and F. Meshkani, "Methane dissociation to CO<sub>x</sub>-free hydrogen and carbon nanofiber over Ni-Cu/Al<sub>2</sub>O<sub>3</sub> catalysts," *Fuel*, 2017, 195, 88-96.
- [74] J. Ashok, P. S. Reddy, G. Raju, M. Subrahmanyam, and A. Venugopal, "Catalytic decomposition of methane to hydrogen and carbon nanofibers over Ni-Cu-SiO<sub>2</sub> catalysts," *Energy & Fuels*, 2008, 23, 5-13.
- [75] S. K. Saraswat and K. Pant, "Synthesis of hydrogen and carbon nanotubes over copper promoted Ni/SiO<sub>2</sub> catalyst by thermocatalytic decomposition of methane," *Journal of Natural Gas Science and Engineering*, 2013, 13, 52-59.
- [76] N. Bayat, M. Rezaei, and F. Meshkani, "Hydrogen and carbon nanofibers synthesis by methane decomposition over Ni-Pd/Al<sub>2</sub>O<sub>3</sub> catalyst," *International Journal of Hydrogen Energy*, 2016, 41, 5494-5503.
- [77] N. Bayat, M. Rezaei, and F. Meshkani, "Methane decomposition over Ni-Fe/Al<sub>2</sub>O<sub>3</sub> catalysts for production of CO<sub>x</sub>-free hydrogen and carbon nanofiber," *International Journal of Hydrogen Energy*, 2016, 41, 1574-1584.
- [78] S. Fangli, S. Meiqing, F. Yanan, W. Jun, and W. Duan, "Influence of supports on catalytic performance and carbon deposition of palladium catalyst for methane partial oxidation," *Journal of Rare Earths*, 2007, 25, 316-320.
- [79] A. Rastegarpanah, F. Meshkani, and M. Rezaei, "CO<sub>x</sub>-free hydrogen and carbon nanofibers production by thermocatalytic decomposition of methane over mesoporous

- MgO· Al<sub>2</sub>O<sub>3</sub> nanopowder-supported nickel catalysts," *Fuel Processing Technology*, 2017, 167,250-262.
- [80] A. Rastegarpanah, F. Meshkani, and M. Rezaei, "Thermocatalytic decomposition of methane over mesoporous nanocrystalline promoted Ni/MgO· Al<sub>2</sub>O<sub>3</sub> catalysts," *International Journal of Hydrogen Energy*,2017, 42, 16476-16488.
- [81] N. Izadi, A. Rashidi, M. Borghei, R. Karimzadeh, and A. Tofigh, "Synthesis of carbon nanofibres over nanoporous Ni–MgO catalyst: influence of the bimetallic Ni–(Cu, Co, Mo) MgO catalysts," *Journal of Experimental Nanoscience*,2012, 7, 160-173.
- [82] J. Li, L. Zhao, J. He, L. Dong, L. Xiong, Y. Du, *et al.*, "Methane decomposition over high-loaded Ni-Cu-SiO<sub>2</sub> catalysts," *Fusion Engineering and Design*, 2016, 113, 279-287.
- [83] K. Srilatha, D. Bhagawan, and V. Himabindu, "Thermo catalytic decomposition of methane over Cu-Al<sub>2</sub>O<sub>3</sub> and 5-20wt% Ni-Cu-Al<sub>2</sub>O<sub>3</sub> catalysts to produce hydrogen and carbon nanofibers," 2016.
- [84] A. E. Awadallah, S. M. Solyman, A. A. Aboul-Enein, H. A. Ahmed, N. A. Aboul-Gheit, and S. A. Hassan, "Effect of combining Al, Mg, Ce or La oxides to extracted rice husk nanosilica on the catalytic performance of NiO during CO<sub>x</sub>-free hydrogen production via methane decomposition," *International Journal of Hydrogen Energy*, 2017, 42, 9858-9872.
- [85] A. H. Fakeeha, A. S. Al-Fatesh, B. Chowdhury, A. A. Ibrahim, W. U. Khan, S. Hassan, *et al.*, "Bi-metallic catalysts of mesoporous Al<sub>2</sub>O<sub>3</sub> supported on Fe, Ni and Mn for Methane decomposition: Effect of activation temperature," *Chinese Journal of Chemical Engineering*, 2018.

- [86] S. K. Saraswat, B. Sinha, K. Pant, and R. B. Gupta, "Kinetic Study and Modeling of Homogeneous Thermocatalytic Decomposition of Methane over a Ni–Cu–Zn/Al<sub>2</sub>O<sub>3</sub> Catalyst for the Production of Hydrogen and Bamboo-Shaped Carbon Nanotubes," *Industrial & Engineering Chemistry Research*, 2016, 55, 11672-11680.
- [87] A. C. Lua and H. Y. Wang, "Hydrogen production by catalytic decomposition of methane over Ni-Cu-Co alloy particles," *Applied Catalysis B: Environmental*, 2014, 156,84-93.
- [88] S. K. Saraswat and K. Pant, "Ni–Cu–Zn/MCM-22 catalysts for simultaneous production of hydrogen and multiwall carbon nanotubes via thermo-catalytic decomposition of methane," *international journal of hydrogen energy*, 2011, 36, 13352-13360.
- [89] S. K. Saraswat and K. Pant, "Synthesis of carbon nanotubes by thermo catalytic decomposition of methane over Cu and Zn promoted Ni/MCM-22 catalyst," *Journal of Environmental Chemical Engineering*, 2013 1, 746-754.
- [90] N. Bayat, F. Meshkani, and M. Rezaei, "Thermocatalytic decomposition of methane to CO<sub>x</sub>-free hydrogen and carbon over Ni–Fe–Cu/Al<sub>2</sub>O<sub>3</sub> catalysts," *International Journal of Hydrogen Energy*, 2016, 41,13039-13049.
- [91] V. V. Chesnokov and A. S. Chichkan, "Production of hydrogen by methane catalytic decomposition over Ni–Cu–Fe/Al<sub>2</sub>O<sub>3</sub> catalyst," *international journal of hydrogen energy*, 2009, 34, 2979-2985.
- [92] M. Pudukudy, Z. Yaakob, and M. S. Takriff, "Methane decomposition over unsupported mesoporous nickel ferrites: effect of reaction temperature on the catalytic activity and properties of the produced nanocarbon," *RSC Advances*, 2016, 6, 68081-68091.

- [93] M. Ermakova, D. Y. Ermakov, G. Kuvshinov, and L. Plyasova, "New nickel catalysts for the formation of filamentous carbon in the reaction of methane decomposition," *Journal of catalysis*, 1999, 187,77-84.
- [94] F. M. Berndt and O. W. Perez-Lopez, "Catalytic decomposition of methane over Ni/SiO<sub>2</sub>: influence of Cu addition," *Reaction Kinetics, Mechanisms and Catalysis*, 2017, 120,181-193.
- [95] A. Konieczny, K. Mondal, T. Wiltowski, and P. Dydo, "Catalyst development for thermocatalytic decomposition of methane to hydrogen," *International Journal of Hydrogen Energy*, 208, 33,264-272.
- [96] M. N. Uddin, W. W. Daud, and H. F. Abbas, "Co-production of hydrogen and carbon nanofibers from methane decomposition over zeolite Y supported Ni catalysts," *Energy Conversion and Management*, 2015, 90, 218-229.
- [97] H. F. Abbas and W. W. Daud, "Thermocatalytic decomposition of methane using palm shell based activated carbon: kinetic and deactivation studies," *Fuel processing technology*, 2009, 90, 1167-1174.
- [98] H. F. Abbas and W. W. Daud, "Thermocatalytic decomposition of methane for hydrogen production using activated carbon catalyst: regeneration and characterization studies," *international journal of hydrogen energy*, 2009, 34,8034-8045.
- [99] J. Pinilla, I. Suelves, R. Utrilla, M. Gálvez, M. Lázaro, and R. Moliner, "Hydrogen production by thermo-catalytic decomposition of methane: regeneration of active carbons using CO<sub>2</sub>," *Journal of power sources*, 2007, 169, 103-109.

- [100] A. Malaika and M. Kozłowski, "Hydrogen production by propylene-assisted decomposition of methane over activated carbon catalysts," *international journal of hydrogen energy*, 2010, 35,10302-10310.
- [101] J. Pinilla, I. Suelves, M. Lázaro, and R. Moliner, "Influence on hydrogen production of the minor components of natural gas during its decomposition using carbonaceous catalysts," *Journal of Power Sources*, 2009192, 100-106.
- [102] A. Malaika and M. Kozłowski, "Influence of ethylene on carbon-catalysed decomposition of methane," *international journal of hydrogen energy*, 2009, 34, 2600-2605.
- [103] A. Malaika, B. Krzyżyńska, and M. Kozłowski, "Catalytic decomposition of methane in the presence of in situ obtained ethylene as a method of hydrogen production," *International journal of hydrogen energy*, 2010, 35, 7470-7475.
- [104] P. Rechnia, A. Malaika, B. Krzyżyńska, and M. Kozłowski, "Decomposition of methane in the presence of ethanol over activated carbon catalyst," *international journal of hydrogen energy*, 2012, 37, 14178-14186.
- [105] P. Rechnia, A. Malaika, L. Najder-Kozdrowska, and M. Kozłowski, "The effect of ethanol on carbon-catalysed decomposition of methane," *international journal of hydrogen energy*, 2012, 37, 7512-7520.
- [106] N. Z. Muradov, "CO<sub>2</sub>-free production of hydrogen by catalytic pyrolysis of hydrocarbon fuel," *Energy & Fuels*, 1998, 12, 41-4.
- [107] A. Adamska, A. Malaika, and M. Kozłowski, "Carbon-catalyzed decomposition of methane in the presence of carbon dioxide," *Energy & Fuels*, vol. 24, pp. 3307-3312, 2010.

- [108] B. Fidalgo, N. Muradov, and J. Menéndez, "Effect of H<sub>2</sub>S on carbon-catalyzed methane decomposition and CO<sub>2</sub> reforming reactions," *international journal of hydrogen energy*, 2012, 37, 14187-14194.
- [109] N. Muradov, F. Smith, and T. Ali, "Catalytic activity of carbons for methane decomposition reaction," *Catalysis Today*, vol. 102, pp. 225-233, 2005.
- [110] A. Erdöhelyi, K. Fodor, and T. Szailer, "Effect of H<sub>2</sub>S on the reaction of methane with carbon dioxide over supported Rh catalysts," *Applied Catalysis B: Environmental*, 2004, 53153-16.
- [111] G. Wang, H. Wang, Z. Tang, W. Li, and J. Bai, "Simultaneous production of hydrogen and multi-walled carbon nanotubes by ethanol decomposition over Ni/Al<sub>2</sub>O<sub>3</sub> catalysts," *Applied Catalysis B: Environmental*, 2009, 88142-15.
- [112] A. Awad, N. Masiran, M. A. Salam, D.-V. N. Vo, and B. Abdullah, "Non-oxidative decomposition of methane/methanol mixture over mesoporous Ni-Cu/Al<sub>2</sub>O<sub>3</sub> Co-doped catalysts," *International Journal of Hydrogen Energy*, 2018.
- [113] M. H. Kim, E. K. Lee, J. H. Jun, S. J. Kong, G. Y. Han, B. K. Lee, *et al.*, "Hydrogen production by catalytic decomposition of methane over activated carbons: kinetic study," *International journal of hydrogen energy*, 2004, 29, 187-193.
- [114] J. Ashok, M. Subrahmanyam, and A. Venugopal, "Hydrotalcite structure derived Ni-Cu-Al catalysts for the production of H<sub>2</sub> by CH<sub>4</sub> decomposition," *International Journal of Hydrogen Energy*, 2008, 33, 2704-2713.
- [115] J. Pinilla, I. Suelves, M. Lázaro, and R. Moliner, "Kinetic study of the thermal decomposition of methane using carbonaceous catalysts," *Chemical Engineering Journal*, 2008, 138, pp. 301-306.

- [116] U. Ashik, W. W. Daud, and H. F. Abbas, "Methane decomposition kinetics and reaction rate over Ni/SiO<sub>2</sub> nanocatalyst produced through co-precipitation cum modified Stöber method," *International Journal of Hydrogen Energy*, 2017, 42, 938-952,.
- [117] H. Y. Wang and A. C. Lua, "Deactivation and kinetic studies of unsupported Ni and Ni–Co–Cu alloy catalysts used for hydrogen production by methane decomposition," *Chemical Engineering Journal*, 2014, 243, 79-91,.
- [118] H. L. Abbott and I. Harrison, "Methane dissociative chemisorption on Ru (0001) and comparison to metal nanocatalysts," *Journal of Catalysis*, 2008, 254, 27-38.
- [119] M. Borghei, R. Karimzadeh, A. Rashidi, and N. Izadi, "Kinetics of methane decomposition to CO<sub>x</sub>-free hydrogen and carbon nanofiber over Ni–Cu/MgO catalyst," *international journal of hydrogen energy*, 2010, 35,9479-9488,.
- [120] I. Kvande, D. Chen, Z. Yu, M. Rønning, and A. Holmen, "Optimization and scale-up of CNF production based on intrinsic kinetic data obtained from TEOM," *Journal of Catalysis*, 2008, 256,204-21.
- [121] S. H. Sharif Zein, A. R. Mohamed, and P. S. Talpa Sai, "Kinetic studies on catalytic decomposition of methane to hydrogen and carbon over Ni/TiO<sub>2</sub> catalyst," *Industrial & engineering chemistry research*, 2004, 43, 4864-487.
- [122] S. Fukada, N. Nakamura, J. Monden, and M. Nishikawa, "Experimental study of cracking methane by Ni/SiO<sub>2</sub> catalyst," *Journal of nuclear materials*, vol. 329, pp. 1365-1369, 2004.
- [123] T. V. Reshetenko, L. B. Avdeeva, Z. R. Ismagilov, A. L. Chuvilin, and V. A. Ushakov, "Carbon capacious Ni-Cu-Al<sub>2</sub>O<sub>3</sub> catalysts for high-temperature methane decomposition," *Applied Catalysis A: General*, 2003: 247,51-63